

Ramification Points of Seiberg-Witten Curves

Chan Y. Park

splendid@caltech.edu

California Institute of Technology

Pasadena, CA 91125, USA

ABSTRACT: When the Seiberg-Witten curve of a four-dimensional $\mathcal{N} = 2$ supersymmetric gauge theory wraps a Riemann surface as a multi-sheeted cover, a topological constraint requires that the curve should develop ramification points that are mapped to branch points on the Riemann surface under the covering map. We show that, while some of the branch points can be identified with the punctures that appear in the work of Gaiotto, in general there are other branch points whose locations on the Riemann surface depend not only on gauge coupling parameters but on Coulomb branch parameters and mass parameters of the theory. We describe how these new branch points can help us to understand interesting physics in various limits of the parameters, including Argyres-Seiberg duality and Argyres-Douglas fixed points.

KEYWORDS: [Seiberg-Witten curve](#), [\$\mathcal{N} = 2\$ supersymmetric gauge theory](#), [Argyres-Seiberg duality](#), [Argyres-Douglas fixed point](#), [normalization](#), [ramification](#), [branch point](#), [Riemann-Hurwitz formula](#).

Contents

1. Introduction	1
2. $SU(2)$ SCFT and the ramification of a Seiberg-Witten curve	3
3. $SU(2) \times SU(2)$ SCFT and a new ramification point	8
4. $SU(3)$ SCFT and Argyres-Seiberg duality	11
5. $SU(3)$ pure gauge theory and Argyres-Douglas fixed points	16
6. $SU(2)$ gauge theory with massive matter	20
6.1 $SU(2)$ gauge theory with four massive hypermultiplets	20
6.2 $SU(2)$ gauge theory with two massive hypermultiplets	23
7. Discussion and outlook	28
A. Normalization of singular algebraic curves	30
B. Compactification of a Seiberg-Witten curve	32
C. Calculation of local normalizations	34
C.1 $SU(2)$ SCFT	34
C.2 $SU(2) \times SU(2)$ SCFT	39
C.3 $SU(3)$ SCFT	43
C.4 $SU(3)$ pure gauge theory	47

1. Introduction

In [1], it was shown that we can describe the Seiberg-Witten curve [2, 3] of a four-dimensional $\mathcal{N} = 2$ supersymmetric field theory by a complex algebraic curve with various parameters of the theory as the coefficients of a polynomial that defines the curve. For example, an $\mathcal{N} = 2$ supersymmetric gauge theory with gauge group $SU(2)$ and four massless hypermultiplets is a superconformal field theory (SCFT) whose Seiberg-Witten curve C_{SW} is given as the zero locus of

$$(t-1)(t-t_1)v^2 - ut, \tag{1.1}$$

where (t, v) is a coordinate of $\mathbb{C}^* \times \mathbb{C}$ that contains C_{SW} , t_1 is related to the marginal gauge coupling parameter of the theory, and u is the Coulomb branch parameter.

In [4], Gaiotto showed that by wrapping N M5-branes over a Riemann surface with punctures, we can get a four-dimensional gauge theory with $\mathcal{N} = 2$ supersymmetry. The locations of the punctures on the Riemann surface describe the gauge coupling parameters of the theory, and each puncture is characterized with a Young tableau of N boxes.

In much the same spirit, we can think of a Seiberg-Witten curve C_{SW} wrapping a Riemann surface C_B in the following way. For C_{SW} that Eq. (1.1) defines, consider t as a coordinate for a base C_B , which is a Riemann sphere in this case, and v as a coordinate normal to C_B . Then the projection $\pi : (v, t) \mapsto t$ gives us the required covering map from C_{SW} to C_B . When we generalize this geometric picture to the case of C_{SW} wrapping C_B N times, one natural way of thinking why each puncture has its Young tableau is to consider a puncture as a branch point of the projection π , which is now an N -sheeted covering map from C_{SW} onto C_B . Then the partition associated to the Young tableau of a puncture shows how the branching of the N sheets occurs there.

Now we can ask a question: can we identify every branch point on C_B that appears in the map $\pi : C_{SW} \rightarrow C_B$ with a puncture in [4]? To answer this question, we will investigate several explicit examples, which will lead us to the conclusion that in general we have new branch points that are not related to the punctures, in addition to the branch points that can be identified with the punctures. And we will illustrate how these branch points can be utilized to explore interesting limits of the various parameters of four-dimensional $\mathcal{N} = 2$ supersymmetric gauge theories.

We start in Section 2 with $SU(2)$ SCFT, where we explain how the covering map π provides the ramification of a Seiberg-Witten curve C_{SW} over a Riemann sphere C_B . In Section 3, we repeat the analysis of Section 2 to study $SU(2) \times SU(2)$ SCFT and find a new ramification point¹ on C_{SW} of this theory whose image under π , or its branch point on C_B , is not related to the punctures of [4]. The location of the new branch point on C_B depends on the Coulomb branch parameters of the theory, unlike the punctures of [4] whose positions are characterized by the gauge coupling parameters only. This enables us to investigate how the new branch point behaves under various limits of the Coulomb branch parameters. In general the locations of these new branch points on C_B depend on every parameter of the gauge theory, including not only gauge coupling parameters but Coulomb branch parameters and mass parameters. To illustrate this, in Section 4 we study $SU(3)$ SCFT and how the branch points behave under the limit of the Argyres-Seiberg duality [5]. In Section 5, we extend the analysis to $SU(3)$ pure gauge theory that is not a SCFT. There we will see how the new branch points help us to identify interesting limits of the Coulomb branch parameters of the theory, the Argyres-Douglas fixed points [6]. In Section 6 we consider $SU(2)$ gauge theories with massive hypermultiplets and illustrate how mass parameters are incorporated

¹When a curve C wraps another curve C' by a covering map $\pi : C \rightarrow C'$, if there is a nontrivial branching of π at $\pi(p) = p' \in C'$ then we say $p \in C$ is a ramification point of C and $p' \in C'$ is a branch point of C' .

in the geometric description of the ramification of C_{SW} . Appendices contain the details of the mathematical procedures and the calculations of the main text.

2. $SU(2)$ SCFT and the ramification of a Seiberg-Witten curve

The first example is four-dimensional $\mathcal{N} = 2$ superconformal $SU(2)$ gauge theory. The corresponding brane configuration in type IIA theory is shown in Figure 1, where a solid line represents a D4-brane and a dashed line represents an NS5-brane.

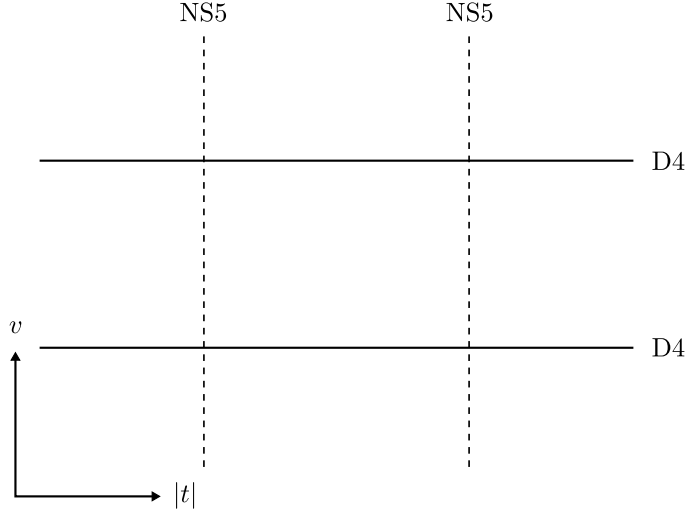


Figure 1: Brane configuration of $SU(2)$ SCFT

After the M-theory lift [1] this brane system becomes an M5-brane that fills the four dimensional spacetime where the field theory lives and wraps the Seiberg-Witten curve. The Seiberg-Witten curve C_{SW} of this theory is described by the zero locus of

$$f(t, v) = (t - 1)(t - t_1)v^2 - ut, \quad (2.1)$$

which is a smooth, non-compact Riemann surface. Note that by construction the following four points

$$(t, v) = (0, 0), (1, \infty), (t_1, \infty), (\infty, 0),$$

are not included in C_{SW} . If we add these four points to the curve, we get a compact algebraic curve \bar{C}_{SW} . The details of how to compactify C_{SW} are explained in Appendix B. \bar{C}_{SW} is guaranteed to be smooth except at the points we added for the compactification, where it can have singularities [7]. Indeed \bar{C}_{SW} has singularities at some of the points we added, and therefore it is not a Riemann surface.

It would be preferable if we can resolve the singularities to find a compact Riemann surface that describes the same physics as C_{SW} . Smoothing out a singular algebraic curve to

find the corresponding Riemann surface can be done by (local) normalization [8, 9, 7]. This means finding a smooth Riemann surface \mathcal{C}_{SW} and a map $\sigma : \mathcal{C}_{SW} \rightarrow \bar{\mathcal{C}}_{SW}, s \mapsto (t(s), v(s))$ around a point of \mathcal{C}_{SW} that is at $s = 0$. Appendix A illustrates how we can get a normalization of a singular curve.

Arguing that \mathcal{C}_{SW} gives the same physics as C_{SW} is a much more difficult question. The answer will depend on the definition of the question, that is, what we mean by “the same physics.” It is very intriguing question but we will not try to address it here.

Now that we have a smooth Riemann surface \mathcal{C}_{SW} , we want to wrap it over a Riemann surface, C_B . Note that for the current example we want C_B to be a Riemann sphere, or \mathbb{CP}^1 , because the corresponding four-dimensional gauge theory comes from a linear quiver brane configuration [4]. One way to express how \mathcal{C}_{SW} wraps \mathbb{CP}^1 is to consider a meromorphic function π on \mathcal{C}_{SW} ,

$$\pi : \mathcal{C}_{SW} \rightarrow \mathbb{CP}^1, s \mapsto t(s).$$

Because π is in general a many-to-one (two-to-one for the current example) mapping, it realizes the required wrapping of \mathcal{C}_{SW} , or its ramification, over \mathbb{CP}^1 . Figure 2 summarizes the whole procedure of getting from C_{SW} its normalization \mathcal{C}_{SW} and finding the ramification of \mathcal{C}_{SW} over C_B .

To analyze the ramification it is convenient to introduce a ramification divisor R_π ,

$$R_\pi = \sum_{s \in \mathcal{C}_{SW}} (\nu_s(\pi) - 1)[s] = \sum_i (\nu_{s_i}(\pi) - 1)[s_i].$$

Here $\nu_s(\pi) \in \mathbb{Z}$ is the ramification index of $s \in \mathcal{C}_{SW}$, $s_i \in \mathcal{C}_{SW}$ is a point where $\nu_{s_i}(\pi) > 1$, and $[s_i]$ is the corresponding divisor² of \mathcal{C}_{SW} . In colloquial language, having a ramification index $\nu_s(\pi)$ at $s \in \mathcal{C}_{SW}$ means that $\nu_s(\pi)$ sheets over C_B is coming together at $\pi(s)$. When $\nu_s(\pi) > 1$ we say s is a ramification point on \mathcal{C}_{SW} , $\pi(s)$ is a branch point on C_B , and $\pi : \mathcal{C}_{SW} \rightarrow C_B$ has a ramification at $\pi(s)$.

The Riemann-Hurwitz formula [8] provides a relation between π , R_π , and the genus of \mathcal{C}_{SW} , $g(\mathcal{C}_{SW})$.

$$\chi_{\mathcal{C}_{SW}} = \deg(\pi) \cdot \chi_{\mathbb{CP}^1} - \deg(R_\pi) \Leftrightarrow \deg(R_\pi) = 2(g(\mathcal{C}_{SW}) + \deg(\pi) - 1). \quad (2.2)$$

Here χ_C is the Euler characteristic of curve C , and $\deg(\pi)$ is the number of intersections of \mathcal{C}_{SW} and $\pi^{-1}(t_0)$ for a general $t_0 \in \mathbb{CP}^1$. In the current example where \mathcal{C}_{SW} is defined as the zero locus of Eq. (2.1), it is easy to see that $\deg(\pi) = 2$ because the equation is quadratic in v . Using this Riemann-Hurwitz formula, we can check if we have found all ramification points that are needed to describe the wrapping of \mathcal{C}_{SW} over C_B .

What we want to know is where the ramification points of \mathcal{C}_{SW} are and what ramification indices they have. We will try to guess where they are by investigating every point $s \in \mathcal{C}_{SW}$ that might have a nontrivial behavior under π . The candidates of such points are

²A divisor is a formal representation of a complex-one-codimension object, a point in this case.

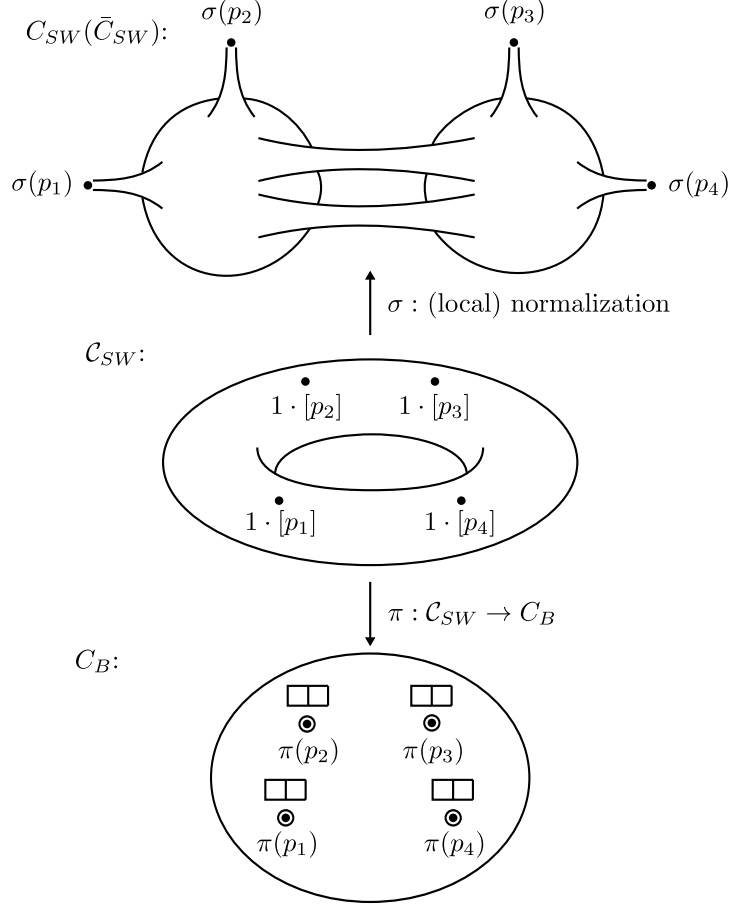


Figure 2: Summary of how to find \mathcal{C}_{SW} and C_B from \mathcal{C}_{SW}

- (1) $\{p_i \in \mathcal{C}_{SW}\}$, where $\sigma(p_i)$'s are the points we added to compactify \mathcal{C}_{SW} ,
- (2) $\{q_i \in \mathcal{C}_{SW} \mid dt(q_i) = 0\} \Leftrightarrow \{q_i \in \mathcal{C}_{SW} \mid (\partial f / \partial v)(t(q_i), v(q_i)) = 0\}$.

Checking the ramification of the points of (1) corresponds to being cautious about π , that is, investigating every point where something nontrivial might happen. Note that $\sigma(p_i)$ is the point where $\lambda = \frac{v}{t} dt$, the Seiberg-Witten differential [10, 11, 12], is singular, and therefore $\pi(p_i)$ corresponds to a puncture of [4]. The reason why the points of (2) correspond to nontrivial ramifications can be illustrated as in Figure 3, which shows two branches of v meeting at $(t(q_i), v(q_i))$.

For the example we are considering now, (1) gives us $\{p_1, p_2, p_3, p_4\}$ such that

$$\sigma(p_1) = (0, 0), \quad \sigma(p_2) = (1, \infty), \quad \sigma(p_3) = (t_1, \infty), \quad \sigma(p_4) = (\infty, 0),$$

and (2) does not give any new point other than (1) provides, so we have $\{p_i\}$ as the candidates to check their ramifications.

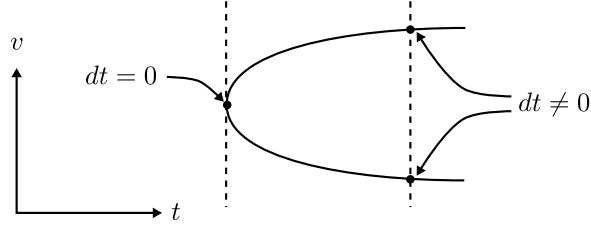


Figure 3: Why a nontrivial ramification occurs at $dt = 0$

Using a local normalization map that is defined around each of these points, we can find the explicit form of π at the neighborhood of the point. If π is just a nice one-to-one mapping near the point, then we can forget about the point. But if π shows a nontrivial ramification at the point, we can describe the ramification of \mathcal{C}_{SW} near the point explicitly and calculate its ramification divisor.

The local normalizations near p_i 's are calculated in Appendix C.1. From the local normalizations we get π , which maps p_i 's to

$$\pi(p_1) = 0, \quad \pi(p_2) = 1, \quad \pi(p_3) = t_1, \quad \text{and} \quad \pi(p_4) = \infty.$$

The ramification divisor of π is also calculated in Appendix C.1,

$$R_\pi = 1 \cdot [p_1] + 1 \cdot [p_2] + 1 \cdot [p_3] + 1 \cdot [p_4], \quad (2.3)$$

which shows that every p_i has nontrivial ramification index of 2, and this is consistent with the Riemann-Hurwitz formula, Eq. (2.2),

$$\deg(R_\pi) = 1 + 1 + 1 + 1 = 4 = 2(g(\mathcal{C}_{SW}) + \deg(\pi) - 1),$$

considering $\deg(\pi) = 2$ and $g(\mathcal{C}_{SW}) = 1$. In the current example, where a Seiberg-Witten curve is given as an elliptic curve, the result of Eq. (2.3) can be expected because an elliptic curve, when considered as a 2-sheeted cover over \mathbb{CP}^1 , has four ramification points of index 2.

To represent what ramification structure each branch point on C_B has, we will decorate it with a Young tableau, which will be constructed in the following way: start with $N = \deg(\pi)$ boxes. Collect the ramification points that are mapped to the same branch point, and put as many boxes as the ramification index of a ramification point in a row. Repeat this to form a row of boxes for each ramification point. Then stack these rows of boxes in an appropriate manner. If we run out of boxes then we are done. If not, then each remaining box is a row by itself, and we stack them too. Figure 4 shows several examples of Young tableaux constructed in this way for various ramification structures.

Figure 5 shows how π maps R_π of \mathcal{C}_{SW} to the branch points of C_B . For this example, all of the branch points are the images of the points $\{p_i\}$ we added to compactify \mathcal{C}_{SW} and each branch point corresponds to a puncture of [4]. Therefore we can say that this example

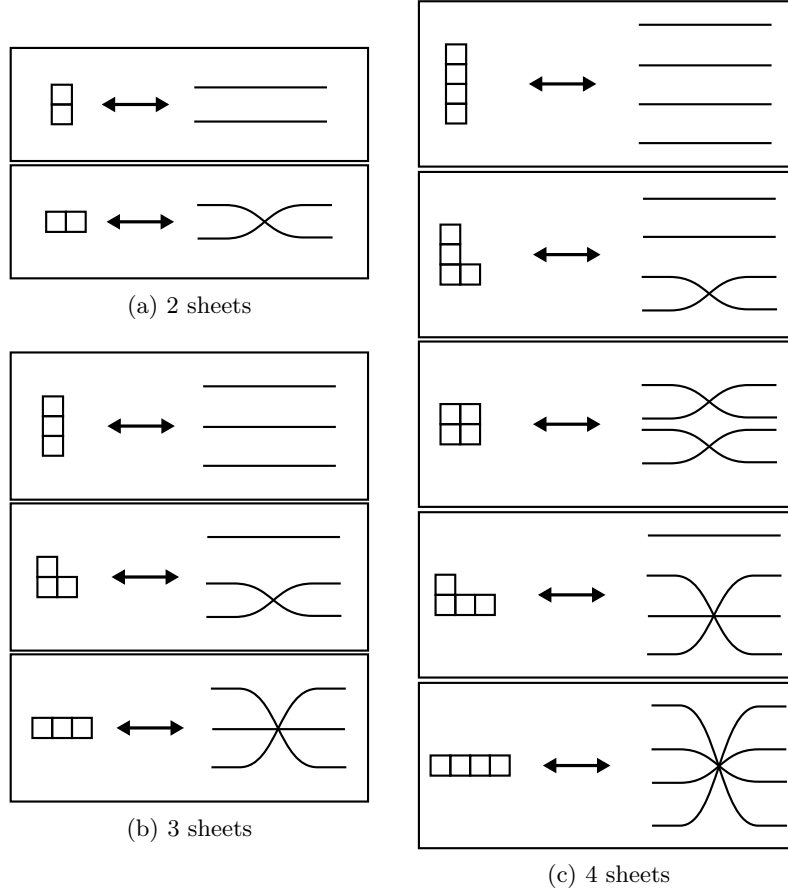


Figure 4: Young tableaux and the corresponding ramification structures

provides a geometric explanation of why each puncture can be labeled with its Young tableau.

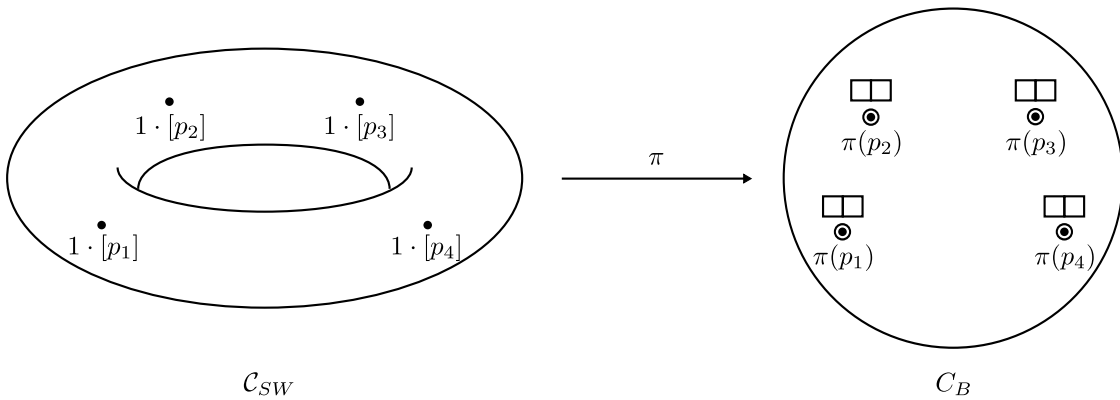


Figure 5: \mathcal{C}_{SW} and \mathcal{C}_B for $SU(2)$ SCFT

A Seiberg-Witten differential $\lambda = \frac{v}{t} dt$ defines a meromorphic 1-form on \mathcal{C}_{SW} . We pull λ back to $\omega = \sigma^*(\lambda)$, which is a meromorphic 1-form on \mathcal{C}_{SW} ³ and therefore should satisfy the Poincaré-Hopf theorem [8]

$$\deg[(\omega)] = 2(g(\mathcal{C}_{SW}) - 1), \quad (2.4)$$

where (ω) is a divisor of ω on \mathcal{C}_{SW} , and $g(\mathcal{C}_{SW})$ is the genus of \mathcal{C}_{SW} . (ω) is defined as

$$(\omega) = \sum_{s \in \mathcal{C}_{SW}} \nu_s(\omega)[s],$$

where $\nu_s(\omega) \in \mathbb{Z}$ is the order⁴ of ω at s .

What we want to do here is to check if Eq.(2.4) holds. In order to do that, we need to find out all the $s \in \mathcal{C}_{SW}$ where $\nu_s(\omega)$ is nonzero. Considering that ω is a pullback of λ , the candidates of such points are

- (1) $\{p_i \in \mathcal{C}_{SW}\}$,
- (2) $\{q_i \in \mathcal{C}_{SW} | dt(q_i) = 0\} \Leftrightarrow \{q_i \in \mathcal{C}_{SW} | (\partial f / \partial v)(t(q_i), v(q_i)) = 0\}$,
- (3) $\{r_i \in \mathcal{C}_{SW} | v(r_i) = 0\}$.

We check (1) because λ is singular at $t(p_i)$ and therefore ω may have a pole at p_i . We also check (2) and (3) because λ vanishes at $t(q_i)$ and $t(r_i)$ and therefore ω may have a zero at q_i or r_i . (3) does not give us any new point for this example, therefore the candidates are $\{p_1, p_2, p_3, p_4\}$, the same set of points we have met when calculating R_π . Using the local normalizations near these points described in Appendix C.1, we get

$$(\omega) = 0,$$

which means ω has neither zero nor pole over \mathcal{C}_{SW} . This is an expected result, since we can find a globally well-defined coordinate z of the elliptic curve \mathcal{C}_{SW} such that $\sigma^*(\lambda) = dz$.

The Poincaré-Hopf theorem, Eq. (2.4), is consistent with the result,

$$\deg[(\omega)] = 0 = 2(g(\mathcal{C}_{SW}) - 1),$$

considering $g(\mathcal{C}_{SW}) = 1$.

3. $SU(2) \times SU(2)$ SCFT and a new ramification point

In Section 2 we have studied four-dimensional $\mathcal{N} = 2$ $SU(2)$ SCFT with a genus 1 Seiberg-Witten curve to identify how the wrapping of \mathcal{C}_{SW} over \mathcal{C}_B can be described by a covering

³To see why it is a meromorphic 1-form on \mathcal{C}_{SW} see Appendix B

⁴When ω has a pole at s , the pole is of order $-\nu_s(\omega)$; when ω has a zero at s , the zero is of order $\nu_s(\omega)$; otherwise $\nu_s(\omega) = 0$.

map π . In this section we apply the analysis to another theory having a Seiberg-Witten curve of genus 2, four-dimensional $\mathcal{N} = 2$ $SU(2) \times SU(2)$ SCFT. From this example, we will learn that there is a ramification point of another kind on \mathcal{C}_{SW} whose image under π cannot be identified with one of the punctures of [4].

Here we repeat the analysis of Section 2 to the brane configuration of Figure 6, which gives four-dimensional $\mathcal{N} = 2$ $SU(2) \times SU(2)$ SCFT. The corresponding Seiberg-Witten curve

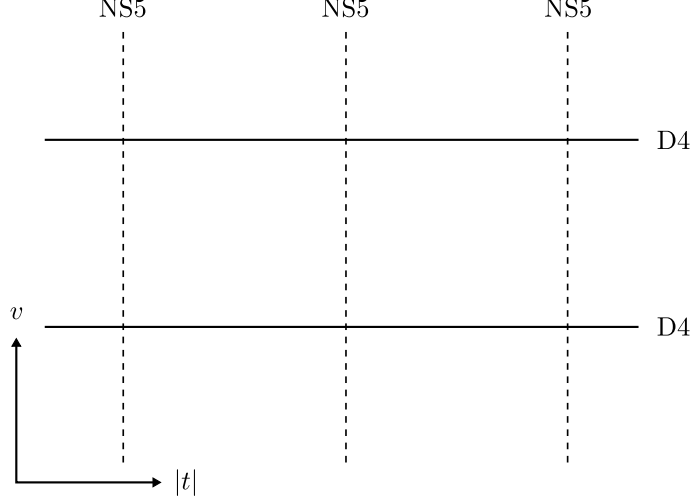


Figure 6: Brane configuration of $SU(2) \times SU(2)$ SCFT

\mathcal{C}_{SW} is the zero locus of

$$f(t, v) = (t - 1)(t - t_1)(t - t_2)v^2 - u_1 t^2 - u_2 t. \quad (3.1)$$

Considering a normalization $\sigma : \mathcal{C}_{SW} \rightarrow \bar{\mathcal{C}}_{SW}$ and a meromorphic function $\pi : \mathcal{C}_{SW} \rightarrow \mathbb{CP}^1$, we can introduce a ramification divisor $R_\pi = \sum_s (\nu_s(\pi) - 1)[s]$. Nontrivial ramifications may occur at

(1) $\{p_i \in \mathcal{C}_{SW}\}$, where $\sigma(p_i)$'s are the points we added to compactify \mathcal{C}_{SW} ,

(2) $\{q_i \in \mathcal{C}_{SW} \mid dt(q_i) = 0\} \Leftrightarrow \{q_i \in \mathcal{C}_{SW} \mid (\partial f / \partial v)(t(q_i), v(q_i)) = 0\}$.

(1) gives us $\{p_i\}$ such that

$$\sigma(p_1) = (0, 0), \quad \sigma(p_2) = (1, \infty), \quad \sigma(p_3) = (t_1, \infty), \quad \sigma(p_4) = (t_2, \infty), \quad \sigma(p_5) = (\infty, 0),$$

and from (2) we get $\{q\}$ such that

$$\sigma(q) = (\rho, 0), \quad \rho = -u_2/u_1.$$

Using the local normalizations calculated in Section C.2, we get

$$R_\pi = 1 \cdot [p_1] + 1 \cdot [p_2] + 1 \cdot [p_3] + 1 \cdot [p_4] + 1 \cdot [p_5] + 1 \cdot [q],$$

and

$$\deg(R_\pi) = 1 + 1 + 1 + 1 + 1 + 1 = 6,$$

which is consistent with the Riemann-Hurwitz formula, Eq. (2.2), considering $\deg(\pi) = 2$ and $g(\mathcal{C}_{SW}) = 2$. Figure 7 shows how π maps \mathcal{C}_{SW} with its ramification points to \mathcal{C}_B with its branch points.

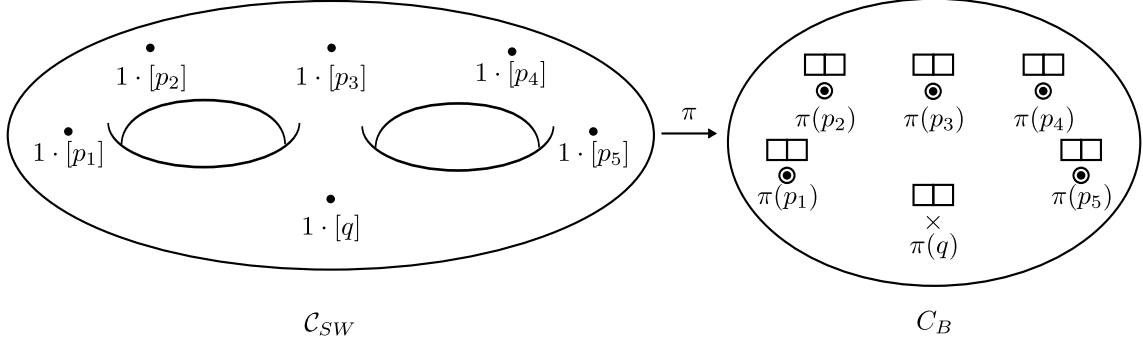


Figure 7: \mathcal{C}_{SW} and \mathcal{C}_B for $SU(2) \times SU(2)$ SCFT

Again R_π has a divisor $[p_i]$ whose image under π can be identified with a puncture of [4]. However, R_π also contains $[q]$, which means that ramification occurs also at q . The location of $\pi(q)$ on \mathcal{C}_B depends on the Coulomb branch parameters u_1 and u_2 , unlike the $\pi(p_i)$'s whose locations depend only on the gauge coupling parameters t_1 and t_2 . We denote the $\pi(q)$ with a symbol different from that of the $\pi(p_i)$'s to distinguish between the two. In the current example, both the $\pi(p_i)$'s and $\pi(q)$ are the branch points of π where two sheets are coming together and therefore each of them has the corresponding Young tableau.

Taking various limits of the Coulomb branch parameters corresponds to moving $\pi(q)$ on \mathcal{C}_B in various ways, as shown in Figure 8. When $\pi(q)$ is infinitesimally away from one of the $\pi(p_i)$'s, imagine cutting out part of the Seiberg-Witten curve that contains the two branch points. As there is no monodromy of $v(t)$ when going around a route that encircles the two branch points, we can fill the excised area topologically with two points, the result of which is the curve shown in the lower right side of Figure 8. This is the curve of $SU(2)$ SCFT that we have investigated in Section 2. And we can complete the excised part by adding two points to it, then that part of the Seiberg-Witten curve separates itself from the rest of the curve to form another curve which has the topology of a sphere. This is the curve shown in the upper right side of Figure 8, where we only represented the ramification structures of the branch points, not identifying the character of each point.

This can also be checked with setting the Coulomb branch parameters to the values corresponding to an appropriate limit and putting them into Eq. (3.1), which will result in a reducible curve with two components, one being the curve of $SU(2)$ SCFT and the other a Riemann sphere when we set $\rho = 1$, t_1 , or t_2 . If we set $\rho = 0$ or ∞ , from the equation we can see only the genus 1 curve.

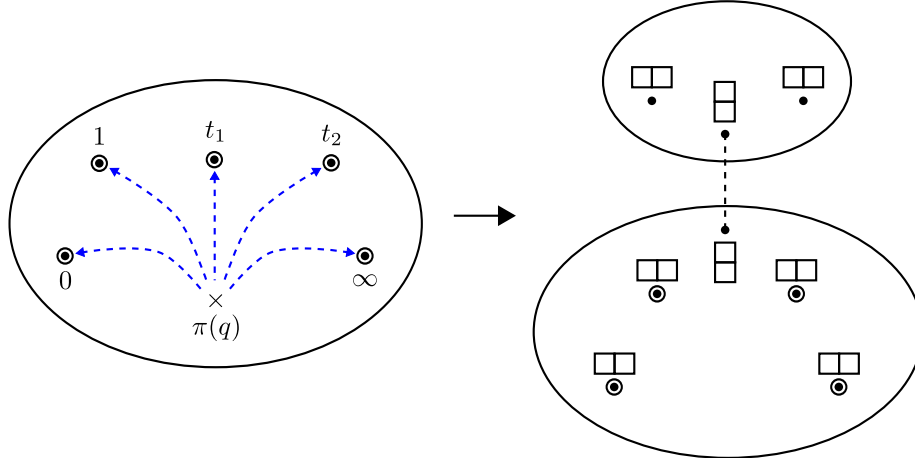


Figure 8: New branch point and the Seiberg-Witten curve under various limits

Now we repeat the same analysis of the Seiberg-Witten differential $\lambda = \frac{v}{t} dt$ that we did in Section 2. The candidates for the points on \mathcal{C}_{SW} where ω has nonzero order are

- (1) $\{p_i \in \mathcal{C}_{SW}\}$,
- (2) $\{q_i \in \mathcal{C}_{SW} | dt(q_i) = 0\} \Leftrightarrow \{q_i \in \mathcal{C}_{SW} | (\partial f / \partial v)(t(q_i), v(q_i)) = 0\}$,
- (3) $\{r_i \in \mathcal{C}_{SW} | v(r_i) = 0\}$.

(3) does not give us any new point for this example, so the candidates are $\{p_i\}$ and $\{q\}$. Again we can analyze how ω behaves near those points by using the local normalizations calculated in Section C.2, which gives

$$(\omega) = 2 \cdot [q],$$

and

$$\deg[(\omega)] = 2 = 2(g(\mathcal{C}_{SW}) - 1).$$

This result is consistent with the Poincaré-Hopf theorem, Eq. (2.4), considering $g(\mathcal{C}_{SW}) = 2$.

4. $SU(3)$ SCFT and Argyres-Seiberg duality

In Section 3 we have found a branch point on C_B that cannot be identified with a puncture. The location of this branch point on C_B depends on the Coulomb branch parameters, which enables us to use it as a tool to describe various limits of the parameters. In this section, we do the same analysis for the example of four-dimensional $\mathcal{N} = 2$ $SU(3)$ SCFT, which will lead us again to the discovery of those new branch points, this time their locations on C_B depending on both the gauge coupling parameters and the Coulomb branch parameters. And

we will see how these branch points help us to illustrate the interesting limit of the theory studied by Argyres and Seiberg [5].

The starting point is four-dimensional $\mathcal{N} = 2$ $SU(3)$ SCFT associated to the brane configuration of Figure 9. The corresponding Seiberg-Witten curve \mathcal{C}_{SW} is defined as the

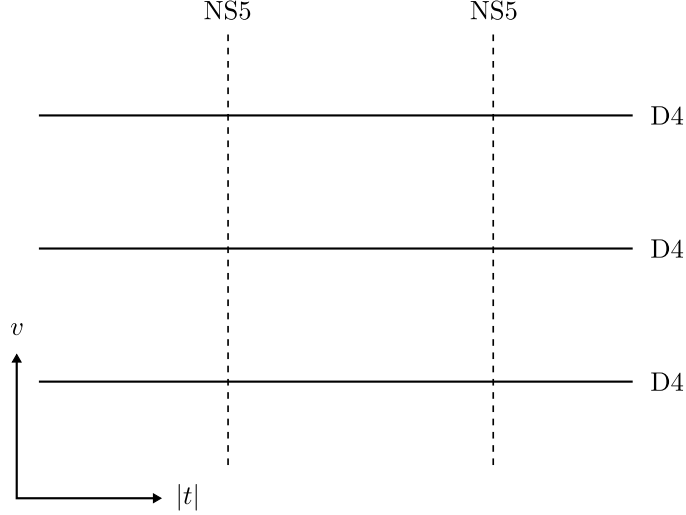


Figure 9: Brane configuration of $SU(3)$ SCFT

zero locus of

$$f(t, v) = (t - 1)(t - t_1)v^3 - u_2tv - u_3t. \quad (4.1)$$

Considering a normalization $\sigma : \mathcal{C}_{SW} \rightarrow \bar{\mathcal{C}}_{SW}$ and a meromorphic function $\pi : \mathcal{C}_{SW} \rightarrow \mathbb{CP}^1$, we can introduce a ramification divisor $R_\pi = \sum_s (\nu_s(\pi) - 1)[s]$. Nontrivial ramifications may occur at

- (1) $\{p_i \in \mathcal{C}_{SW}\}$, where $\sigma(p_i)$'s are the points we added to compactify \mathcal{C}_{SW} ,
- (2) $\{q_i \in \mathcal{C}_{SW} \mid dt(q_i) = 0\} \Leftrightarrow \{q_i \in \mathcal{C}_{SW} \mid (\partial f / \partial v)(t(q_i), v(q_i)) = 0\}$.

From (1) we get $\{p_i\}$ such that

$$\sigma(p_1) = (0, 0), \quad \sigma(p_2) = (1, \infty), \quad \sigma(p_3) = (t_1, \infty), \quad \sigma(p_4) = (\infty, 0).$$

(2) gives us $\{q_\pm\}$ such that

$$\sigma(q_\pm) = (t_\pm, v_0),$$

where

$$v_0 = -\frac{(u_3/2)}{(u_2/3)}$$

and t_{\pm} are the two roots of the equation $f(t, v_0) = 0$ in t ,

$$t_{\pm} = \frac{1 + t_1 + \rho}{2} \pm \sqrt{\left(\frac{1 + t_1 + \rho}{2}\right)^2 - t_1}, \quad \rho = \frac{(u_2/3)^3}{(u_3/2)^2}.$$

Calculations for the local normalizations near the points are given in Appendix C.3, from which we get the ramification divisor of π as

$$R_{\pi} = 2 \cdot [p_1] + 1 \cdot [p_2] + 1 \cdot [p_3] + 2 \cdot [p_4] + 1 \cdot [q_+] + 1 \cdot [q_-],$$

and this satisfies

$$\deg(R_{\pi}) = 2 + 1 + 1 + 2 + 1 + 1 = 8 = 2(g(\mathcal{C}_{SW}) + \deg(\pi) - 1),$$

which is consistent with the Riemann-Hurwitz formula, Eq. (2.2), considering $\deg(\pi) = 3$ and $g(\mathcal{C}_{SW}) = 2$.

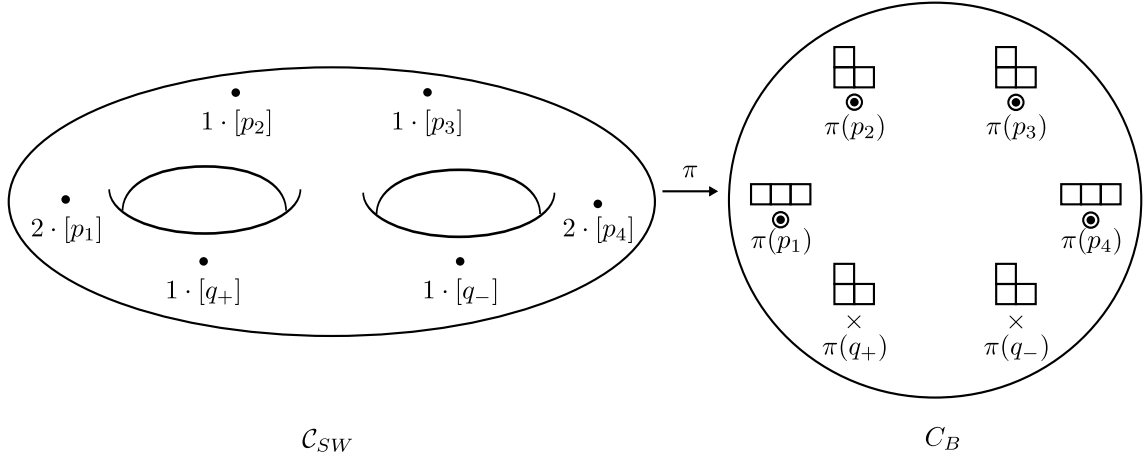


Figure 10: \mathcal{C}_{SW} and \mathcal{C}_B for $SU(3)$ SCFT

Considering that π is in general three-to-one mapping, the fact that R_{π} has degree 2 at p_1 implies that the three sheets are coming together at $\pi(p_1)$, which corresponds to a Young tableau $\square\square\square$. And R_{π} having degree 1 at p_2 is translated into only two out of three sheets coming into contact at $\pi(p_2)$, which corresponds to a Young tableau $\square\square$. R_{π} also contains $[q_{\pm}]$, which means that ramifications occur also at q_{\pm} . These are the points of \mathcal{C}_{SW} where $dt = 0$ along the curve. The locations of $\pi(q_{\pm})$ on \mathcal{C}_B depend on both gauge coupling parameter t_1 and Coulomb branch parameters u_2 and u_3 , unlike the $\pi(p_i)$'s whose locations depend only on t_1 . Figure 10 shows how π works.

To investigate how the Argyres-Seiberg duality [5] is illustrated by the new branch points, we take the corresponding limits for the Coulomb branch parameters and the gauge coupling parameter. When we take $u_2 \rightarrow 0$, $\pi(q_+)$ and $\pi(q_-)$ move toward $\pi(p_2) = 1$ and $\pi(p_3) = t_1$,

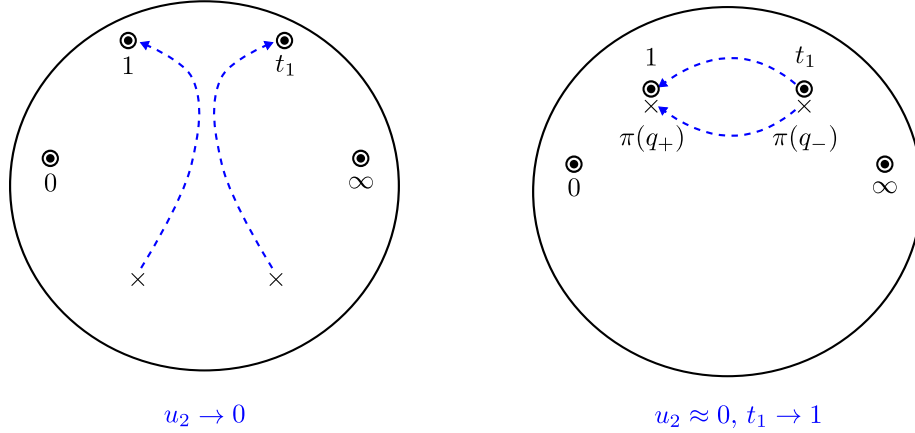


Figure 11: Behaviors of the branch points under the limit $u_2 \rightarrow 0$ and $t_1 \rightarrow 1$

respectively. In addition we take the limit of $t_1 \rightarrow 1$, and the four branch points come together. Figure 11 shows the behavior of the branch points under the limit of the parameters. When we are near the limit of $u_2 = 0$ and $t_1 = 1$, the four branch points become infinitesimally separated from one another and we can imagine cutting out the part of the Seiberg-Witten curve that contains the four branch points, separating the original curve into two parts. As the monodromy of $v(t)$ around the four branch points indicates that we can complete both parts by adding a point of ramification index 3 to each of them, we can see that the one part becomes a genus 1 curve and the other becomes another genus 1 curve after the completion of the two. Figure 12 illustrates this. The genus 1 curve with three branch points of ramification

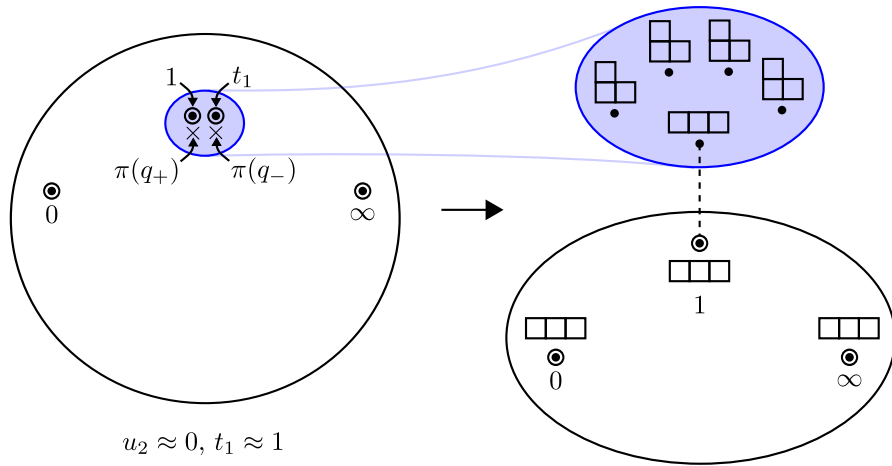


Figure 12: Appearance of E_6 curve under the limit $u_2 \rightarrow 0$ and $t_1 \rightarrow 1$

index 3 corresponds to the zero locus of

$$(t - 1)^2 v^3 - u_3 t,$$

which is from Eq. (4.1) by setting $t_1 = 1$ and $u_2 = 0$. This curve can be identified with the Seiberg-Witten curve of E_6 theory [5, 4]. The other genus 1 curve is a small torus, which reminds us of the weakly gauged $SU(2)$ theory coupled to the E_6 theory that appears in [5, 4].

When we take $u_3 \rightarrow 0$ limit, $\pi(q_+)$ and $\pi(q_-)$ move toward $\pi(p_1) = 0$ and $\pi(p_4) = \infty$, respectively. The collision of $\pi(q_+)$ with $\pi(p_1)$ unravels part of the ramification over the two branch points, which results in one branch point with the corresponding ramification point having index 2, and the third sheet falling apart from the branch point. The same thing happens at $t = \infty$, so the result of the limit is a reducible curve with two components, one component being the same $SU(2)$ SCFT curve that we have investigated in Section 2 and the other a Riemann sphere. This can also be checked by setting $u_3 = 0$ in Eq. (4.1), which gives us a $SU(2)$ SCFT curve and a Riemann sphere. Figure 13 illustrates the limit and the partial unraveling of the ramification.

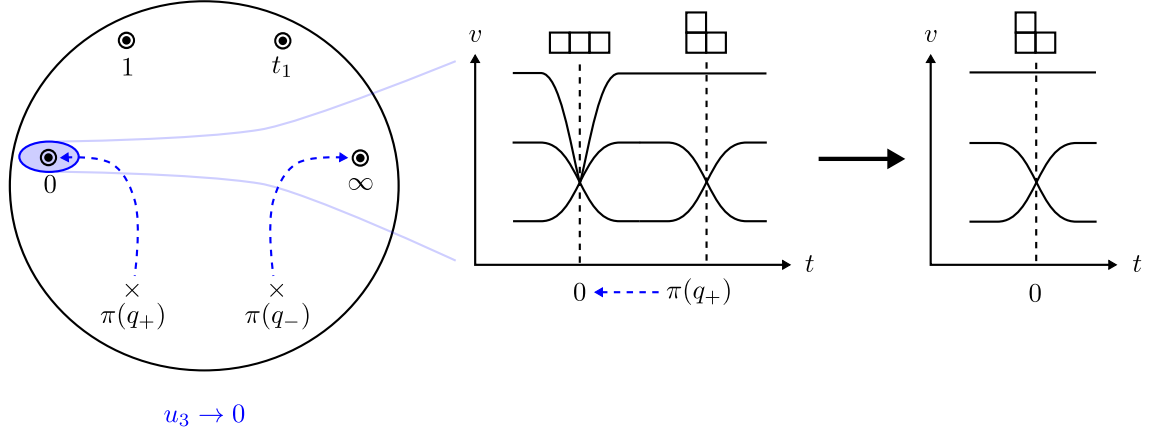


Figure 13: Behaviors of the new branch points under the limit $u_3 \rightarrow 0$

Let's proceed to the calculation of $(\omega) = \sum_s \nu_s(\omega)[s]$. The candidates for the points on \mathcal{C}_{SW} where ω has nonzero order are

- (1) $\{p_i \in \mathcal{C}_{SW}\}$,
- (2) $\{q_i \in \mathcal{C}_{SW} | dt(q_i) = 0\} \Leftrightarrow \{q_i \in \mathcal{C}_{SW} | (\partial f / \partial v)(t(q_i), v(q_i)) = 0\}$,
- (3) $\{r_i \in \mathcal{C}_{SW} | v(r_i) = 0\}$.

(1) and (2) give us $\{p_i\}$ and $\{q_{\pm}\}$, respectively. (3) does not result in any new point. Using the local normalizations calculated in Appendix C.3, we can get

$$(\omega) = 1 \cdot [q_+] + 1 \cdot [q_-],$$

which is consistent with the Poincaré-Hopf theorem, Eq. (2.4),

$$\deg[(\omega)] = 1 + 1 = 2 = 2(g(\mathcal{C}_{SW}) - 1),$$

considering $g(\mathcal{C}_{SW}) = 2$.

5. $SU(3)$ pure gauge theory and Argyres-Douglas fixed points

What is interesting about the new branch points we have found in Sections 3 and 4 is that their locations on C_B depend in general on every parameter of the Seiberg-Witten curve, including both gauge coupling parameters and Coulomb branch parameters. Therefore they can be useful in analyzing how a Seiberg-Witten curve behaves as we take various limits for the parameters.

Furthermore, considering that branch points are important to understand various noncontractible 1-cycles of a curve and that each such cycle on a Seiberg-Witten curve corresponds to a BPS state with its mass given by the integration of the Seiberg-Witten differential along the cycle, the behaviors of branch points under the various limits of the parameters may tell us some information regarding the BPS states.

To expand on these ideas, we will investigate in this section the case of four-dimensional $\mathcal{N} = 2$ $SU(3)$ pure gauge theory, where there are special limits of the Coulomb branch parameters, the Argyres-Douglas fixed points [6]. We will describe how the new branch points help us to identify the small torus that arises at the fixed points in the study of Argyres and Douglas.

Here the starting point is a four-dimensional $\mathcal{N} = 2$ $SU(3)$ pure gauge theory associated to the brane configuration of Figure 14. Corresponding Seiberg-Witten curve \mathcal{C}_{SW} is given

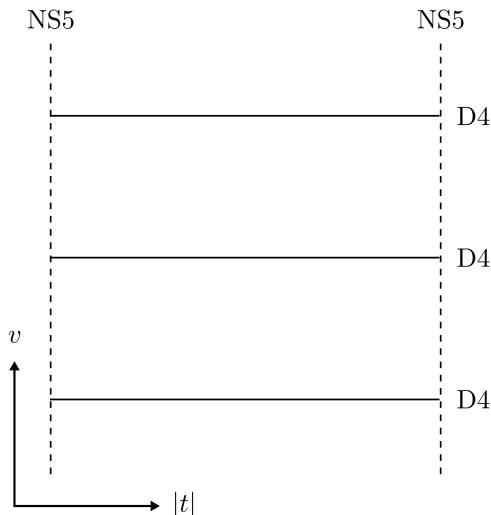


Figure 14: Brane configuration of $SU(3)$ pure gauge theory

by the zero locus of

$$\tilde{f}(t, v) = t^2 + (v^3 - u_2v - u_3)t + \Lambda^6,$$

where Λ is the dynamically generated scale of the corresponding four-dimensional theory. This is different from the previous examples, where the corresponding four-dimensional theories are conformal and therefore are scale-free. To avoid cluttered notations, let's rescale the variables in the following way:

$$\frac{t}{\Lambda^3} \rightarrow t, \quad \frac{v}{\Lambda} \rightarrow v, \quad \frac{u_k}{\Lambda^k} \rightarrow u_k. \quad (5.1)$$

It is easy to restore the scale if needed, just reversing the direction of the rescaling. Then the equation that we start the usual analysis with is

$$f(t, v) = t^2 + (v^3 - u_2v - u_3)t + 1 = tv^3 - u_2tv + (t^2 - u_3t + 1)$$

whose zero locus defines \mathcal{C}_{SW} .

Considering a normalization $\sigma : \mathcal{C}_{SW} \rightarrow \bar{\mathcal{C}}_{SW}$ and a meromorphic function $\pi : \mathcal{C}_{SW} \rightarrow \mathbb{CP}^1$, we can introduce a ramification divisor $R_\pi = \sum_s (\nu_s(\pi) - 1)[s]$. Nontrivial ramifications may occur at

- (1) $\{p_i \in \mathcal{C}_{SW}\}$, where $\sigma(p_i)$'s are the points we added to compactify \mathcal{C}_{SW} ,
 - (2) $\{q_i \in \mathcal{C}_{SW} \mid dt(q_i) = 0\} \Leftrightarrow \{q_i \in \mathcal{C}_{SW} \mid (\partial f / \partial v)(t(q_i), v(q_i)) = 0\}$.
- (1) gives us $\{p_1, p_2\}$ such that

$$\sigma(p_1) = (0, \infty), \quad \sigma(p_2) = (\infty, \infty),$$

and (2) gives us $\{q_{\pm\pm}\}$ such that

$$\sigma(q_{ab}) = (t_{2ab}, v_{2a}),$$

where $a, b = \pm 1$, $v_{2a} = a\sqrt{u_2/3}$, and t_{2ab} are the two roots of $f(t, v_{2a}) = 0$,

$$t_{2ab} = \left(v_{2a}^3 + \frac{u_3}{2}\right) + b\sqrt{\left(v_{2a}^3 + \frac{u_3}{2}\right)^2 - 1}.$$

Using the local normalizations calculated in Section C.4, we get

$$R_\pi = 2 \cdot [p_1] + 2 \cdot [p_2] + 1 \cdot [q_{++}] + 1 \cdot [q_{+-}] + 1 \cdot [q_{-+}] + 1 \cdot [q_{--}],$$

and considering $\deg(\pi) = 3$ and $g(\mathcal{C}_{SW}) = 2$,

$$\deg(R_\pi) = 8 = 2(g(\mathcal{C}_{SW}) + \deg(\pi) - 1)$$

is consistent with the Riemann-Hurwitz formula, Eq. (2.2). Figure 15 illustrates how π works for this example.

The divisor of $\omega = \sigma^*(\lambda)$ is $(\omega) = \sum_s \nu_s(\omega)[s]$, and the candidates for the points on \mathcal{C}_{SW} where ω has nonzero order are

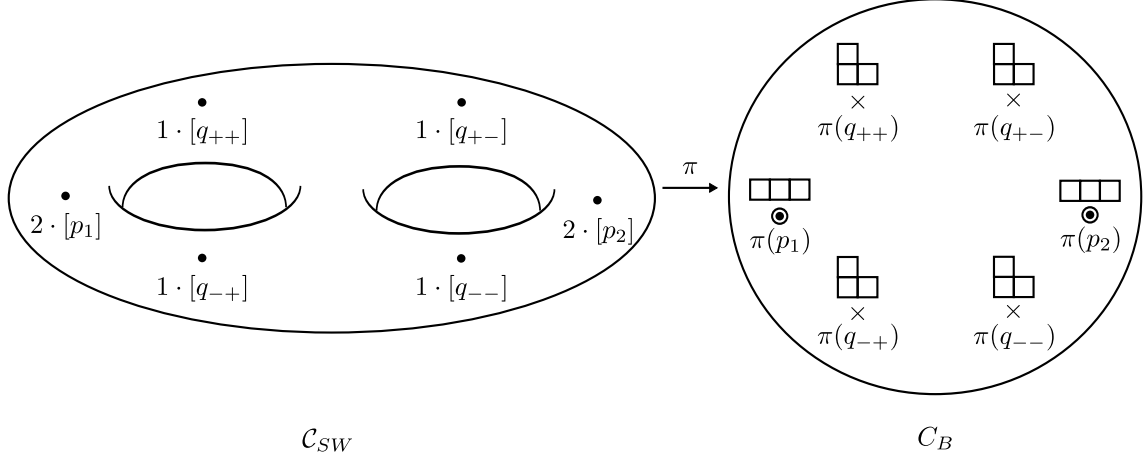


Figure 15: \mathcal{C}_{SW} and \mathcal{C}_B for $SU(3)$ pure gauge theory

- (1) $\{p_i \in \mathcal{C}_{SW}\}$,
- (2) $\{q_i \in \mathcal{C}_{SW} | dt(q_i) = 0\} \Leftrightarrow \{q_i \in \mathcal{C}_{SW} | (\partial f / \partial v)(t(q_i), v(q_i)) = 0\}$,
- (3) $\{r_i \in \mathcal{C}_{SW} | v(r_i) = 0\}$.

(1) and (2) result in $\{p_1, p_2\}$ and $\{q_{ab}\}$, respectively. (3) gives us $\{r_{\pm}\}$ such that

$$\sigma(r_{\pm}) = (t_{3\pm}, 0),$$

where $t_{3\pm}$ are the two roots of $f(t, 0) = 0$. Using the local normalizations calculated in Appendix C.4, we can get

$$(\omega) = -2 \cdot [p_1] - 2 \cdot [p_2] + 1 \cdot [q_{++}] + 1 \cdot [q_{+-}] + 1 \cdot [q_{-+}] + 1 \cdot [q_{--}] + 1 \cdot [r_+] + 1 \cdot [r_-],$$

which is consistent with the Poincaré-Hopf theorem, Eq. (2.4),

$$\deg[(\omega)] = 2 = 2(g(\mathcal{C}_{SW}) - 1),$$

considering $g(\mathcal{C}_{SW}) = 2$.

Now let's go back to the consideration of the ramification of the Seiberg-Witten curve. As the Argyres-Douglas fixed points are at $u_2 = 0$ and $u_3 = \pm 2$, let's denote the deviations from one of the Coulomb branch points by

$$u_2 = 0 + \delta u_2 = 3\epsilon^2 \rho, \tag{5.2}$$

$$u_3 = 2 + \delta u_3 = 2 + 2\epsilon^3, \tag{5.3}$$

where we picked $u_3 = 2$ for convenience. Then $\pi(q_{ab}) = t_{2ab}$ are, when $\epsilon \ll 1$,

$$t_{2ab} \approx 1 + b\sqrt{2(1 + a\rho^{3/2})}\epsilon^3. \tag{5.4}$$

When ϵ is infinitesimal, these points gather together near $t = 1$, away from the $\pi(p_i)$'s. The four values of t_{2ab} are away from $t = 1$ by the distance of order $\mathcal{O}(\epsilon^{3/2})$. Figure 16 illustrates this Coulomb branch limit.

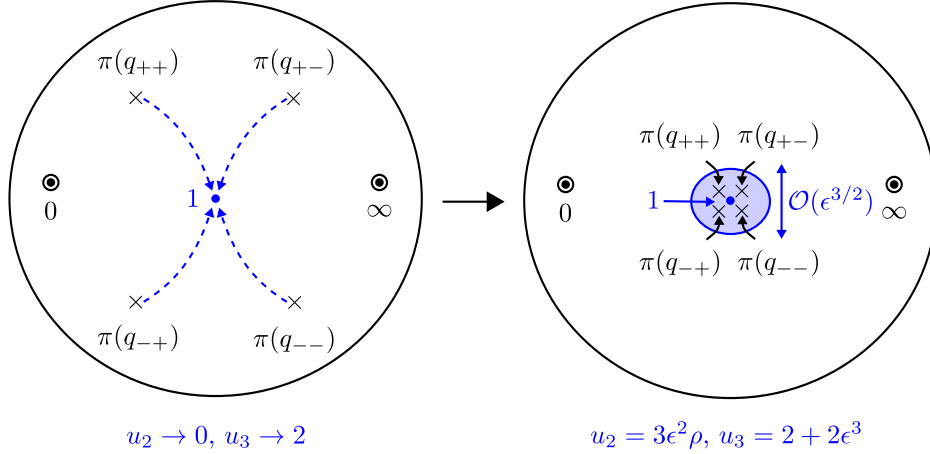


Figure 16: Behaviors of the new branch points near the Argyres-Douglas fixed point

From the viewpoint of the ramification structure of the Seiberg-Witten curve, this is a similar situation that we have seen in Section 4, where we cut a Seiberg-Witten curve into two parts and completed each of them by adding a point of ramification index 3. We do the same thing here, thereby getting a genus 1 curve, which is a small torus, and another genus 1 curve whose Seiberg-Witten curve is the zero locus of

$$v^3t + (t - 1)^2,$$

which is the curve with three branch points of ramification index 3. But this time we will try to find out the algebraic equation that describes the small torus. For that purpose it is tempting to zoom in on the part of C_B near $t = 1$, in such a way that every parameter has an appropriate dependence on ϵ so that we can cancel out ϵ from all of the parameters. Considering Eqs. (5.1), (5.2), (5.3) and (5.4), a natural way to scale out ϵ is to redefine the variables as

$$\begin{aligned} v &= \epsilon\sigma, \\ u_2 &= 0 + 3\epsilon^2\rho, \\ u_3 &= 2 + 2\epsilon^3 \\ t &= 1 + i\epsilon^{3/2}\tau. \end{aligned}$$

Then $f(t, v)$ becomes

$$\begin{aligned} f(t, v) &= (t - 1)^2 + \epsilon^3(\sigma^3 - 3\sigma\rho - 2)t \\ &\approx (-\tau^2 + \sigma^3 - 3\sigma\rho - 2)\epsilon^3 + \mathcal{O}(\epsilon^{9/2}), \end{aligned}$$

where we can identify a torus given by $\tau^2 = \sigma^3 - 3\sigma\rho - 2$, the same torus that appears at the Argyres-Douglas fixed points [6]. Figure 17 illustrates this procedure.

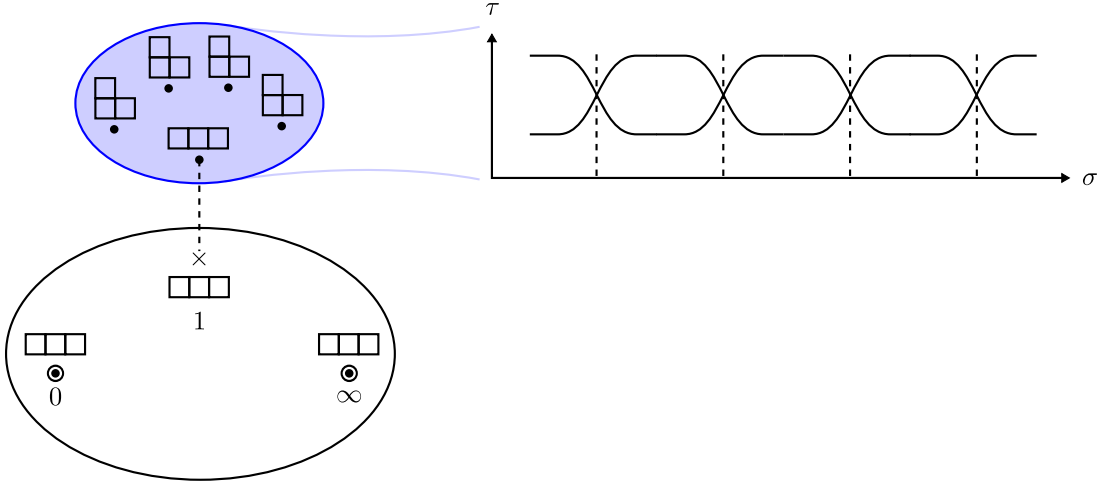


Figure 17: Appearance of a small torus at the Argyres-Douglas fixed points

We can also calculate the Seiberg-Witten differential $\lambda = \frac{v}{t} dt$ on the torus,

$$\lambda = \frac{v}{t} dt \approx \frac{\epsilon\sigma}{1} \cdot i\epsilon^{3/2} d\tau = i\epsilon^{5/2} \sigma d\tau,$$

which agrees with the Seiberg-Witten differential that is calculated in [6].

6. $SU(2)$ gauge theory with massive matter

In this section we will take a look at the cases of four-dimensional $\mathcal{N} = 2$ $SU(2)$ gauge theories with massive hypermultiplets, where we can observe interesting limits of the Coulomb branch parameters and the mass parameters [13].

6.1 $SU(2)$ gauge theory with four massive hypermultiplets

In section 2 we analyzed four-dimensional $\mathcal{N} = 2$ $SU(2)$ SCFT, which has four massless hypermultiplets. Here we examine the theory with the same amount of supersymmetry and the same gauge group but with massive hypermultiplets, and see how additional mass parameters change the ramification structure of the Seiberg-Witten curve.

This gauge theory is associated to the brane configuration of Figure 18. Corresponding Seiberg-Witten curve C_{SW} is given by the zero locus of

$$f(t, v) = (v - m_1)(v - m_3)t^2 - (v^2 - u_2)t + (v - m_2)(v - m_4)c_4, \quad (6.1)$$

where m_1 and m_3 are the mass parameters of the hypermultiplets at $t = \infty$, m_2 and m_4 are the mass parameters of the hypermultiplets at $t = 0$, u_2 is the Coulomb branch parameter,

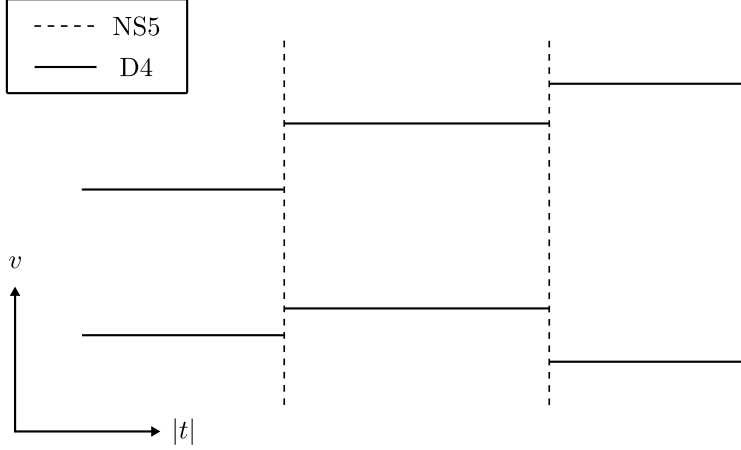


Figure 18: Brane configuration of $SU(2)$ gauge theory with four massive hypermultiplets

and c_4 corresponds to the dimensionless gauge coupling parameter that cannot be absorbed by rescaling t and v [1].

From the usual analysis we get C_B with its branch points as shown in Figure 19.

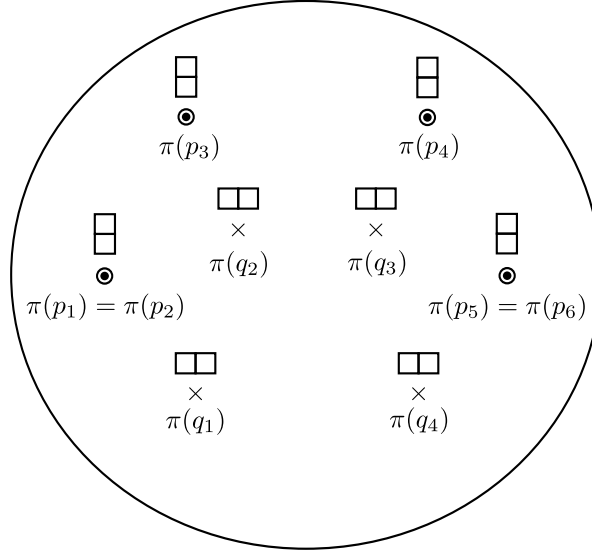


Figure 19: C_B for $SU(2)$ gauge theory with four massive hypermultiplets

Here p_i 's are the points on C_{SW} such that

$$\begin{aligned} \sigma(p_1) &= (0, m_2), \quad \sigma(p_2) = (0, m_4), \quad \sigma(p_3) = (t_-, \infty), \quad \sigma(p_4) = (t_+, \infty), \\ \sigma(p_5) &= (\infty, m_1), \quad \sigma(p_6) = (\infty, m_3), \quad t_{\pm} = \frac{1}{2} (1 \pm \sqrt{1 - 4c_4}) \end{aligned}$$

are the points we added to C_{SW} to compactify it. q_i 's are where $dt(q_i) = 0$ and whose images under π are the four roots of

$$\begin{aligned} & \frac{1}{4}(m_1 - m_3)^2 t^4 + (m_1 m_3 - u_2) t^3 + \\ & + \frac{1}{2} [c_4 (m_1 m_2 + m_2 m_3 + m_3 m_4 + m_4 m_1 - 2m_1 m_3 - 2m_2 m_4) + 2u_2] t^2 + \\ & + c_4 (m_2 m_4 - u_2) t + \frac{1}{4} c_4^2 (m_2 - m_4)^2. \end{aligned}$$

One notable difference from the previous examples is that $\pi(p_i)$'s are not branch points, although $\lambda = \frac{v}{t} dt$ is still singular there. Instead we have four branch points $\{\pi(q_i)\}$ which furnish the required ramification structure. We can see that the locations of the branch points now depend also on the mass parameters in addition to the gauge coupling parameter and the Coulomb branch parameter.

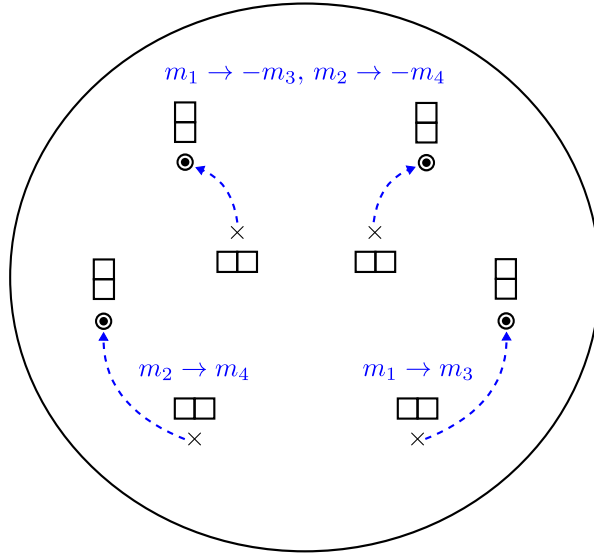


Figure 20: Behaviors of the branch points under various limits of mass parameters

This theory has four more parameters, $\{m_i\}$, when compared to $SU(2)$ SCFT. In some sense, these mass parameters represent possible deformations of the Seiberg-Witten curve of $SU(2)$ SCFT. To understand what the deformations are, let's first see how $\pi(q_i)$'s move when we take various limits of the mass parameters.

1. When $m_1 \rightarrow m_3$, one of $\pi(q_i)$'s, say $\pi(q_4)$, moves to $t = \infty = \pi(p_5) = \pi(p_6)$.
2. When $m_2 \rightarrow m_4$, one of $\pi(q_i)$'s, say $\pi(q_1)$, moves to $t = 0 = \pi(p_1) = \pi(p_2)$.
3. When $m_1 \rightarrow -m_3$ and at the same time $m_2 \rightarrow -m_4$, $\pi(q_2)$ moves to $t = t_- = \pi(p_3)$ and $\pi(q_3)$ moves to $t = t_+ = \pi(p_4)$.

The first limit corresponds to bringing the two endpoints of \bar{C}_{SW} at $t = \infty$, p_5 and p_6 , together to one point, thereby developing a ramification point of index 2 there. The others can also be understood in a similar way. Figure 20 illustrates these limits. Note that we can get the Seiberg-Witten curve of $SU(2)$ SCFT by setting all the mass parameters of Eq. (6.1) to zero, which corresponds to the limit where we take all three of the limits at the same time, thereby sending $\pi(q_i)$'s to $\pi(p_i)$'s and making them the four branch points as expected.

Now we turn the previous arguments on its head and see how we can deform the Seiberg-Witten curve of $SU(2)$ SCFT by turning on mass parameters. As an example, let's consider turning on $m_1 = -m_3 = m$. When $m = 0$, there is a branch point at $t = 0$. Now we turn m on, then this separates the two sheets at $t = 0$, and $t = 0$ is no longer a branch point. But the topological constraint by Riemann-Hurwitz formula requires four branch points to exist, and indeed a new branch point that corresponds to $\pi(q_1)$ develops. Figure 21 illustrates this deformation. The other mass parameters can also be understood in a similar way as

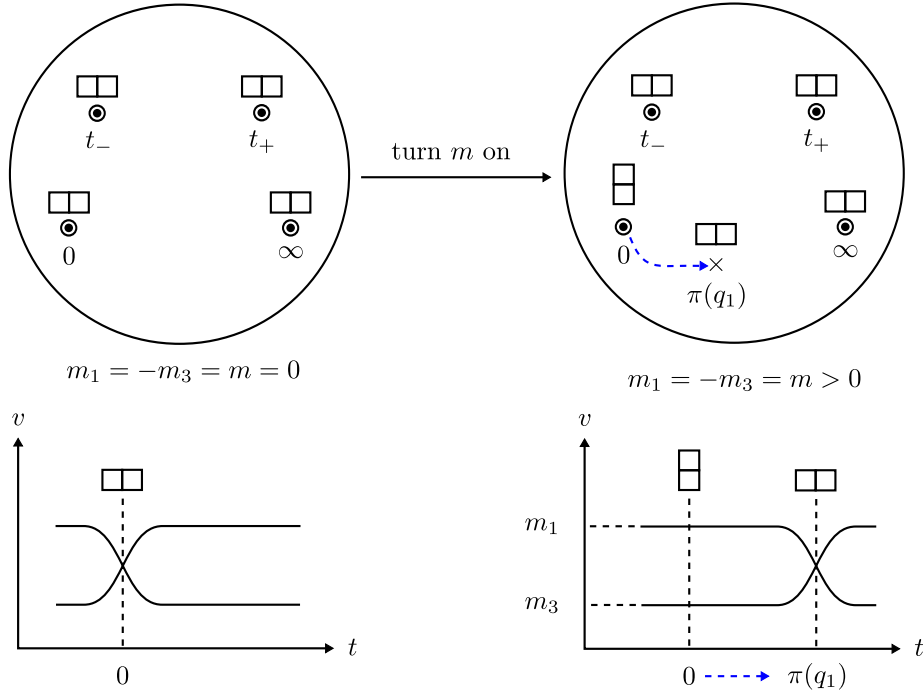


Figure 21: Removal of the branch point at $t = 0$ when we turn $m_1 = -m_3 = m$ on

deformations that detach the sheets meeting at the branch points from each other, and the most general deformation will result in the Seiberg-Witten curve of $SU(2)$ gauge theory with four massive hypermultiplets, the theory we started our analysis here.

6.2 $SU(2)$ gauge theory with two massive hypermultiplets

Now we examine the example of four-dimensional $\mathcal{N} = 2$ supersymmetric $SU(2)$ gauge theory with two massive hypermultiplets. One interesting point of this theory is that there is an

ambiguity in constructing the brane configuration associated to the theory. One possible brane configuration is shown in Figure 22, where two D4-branes that provide the massive hypermultiplets are distributed symmetrically on both sides.

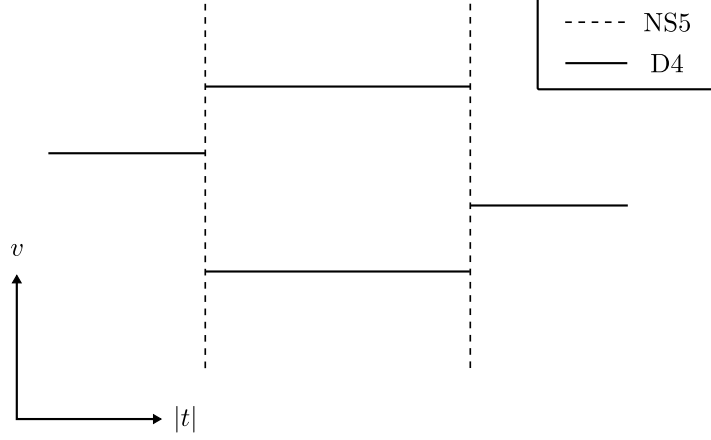


Figure 22: Brane configuration of $SU(2)$ gauge theory with two massive hypermultiplets, with symmetric distribution of D4-branes

Corresponding Seiberg-Witten curve C_{SW} is given by the zero locus of

$$\tilde{f}(t, v) = (v - m_1)t^2 - (v^2 - u_2)t + (v - m_2)\Lambda_2^2, \quad (6.2)$$

where u_2 is the Coulomb branch parameter, m_1 and m_2 are the mass parameters, and Λ_2 is the dynamically generated scale of the theory, with a subscript of 2 to remind us of the fact that this theory has two massive hypermultiplets.

The usual analysis gives C_B and its branch points as shown in Figure 23. p_1 and p_2 are the points on C_{SW} such that

$$\sigma(p_1) = (0, \infty), \quad \sigma(p_2) = (\infty, \infty), \quad (6.3)$$

are the points we add to C_{SW} to compactify it. Note that here $\pi(p_1) = 0$ and $\pi(p_2) = \infty$ are not branch points. There are four branch points $\{\pi(q_i)\}$ whose locations on C_B are given as the four roots $\{t_i\}$ of the following equation.

$$\frac{1}{4}t^4 - m_1t^3 + \left(u_2 + \frac{\Lambda_2^2}{2}\right)t^2 - m_2\Lambda_2^2t + \frac{\Lambda_2^4}{4}.$$

Therefore we can see that the locations of the new branch points now depend also on the mass parameters in addition to the Coulomb branch parameter and the scale.

When we take the following limits for the parameters,

$$m_1 = m_2 \rightarrow \Lambda_2, \quad u_2 \rightarrow \Lambda_2^2,$$

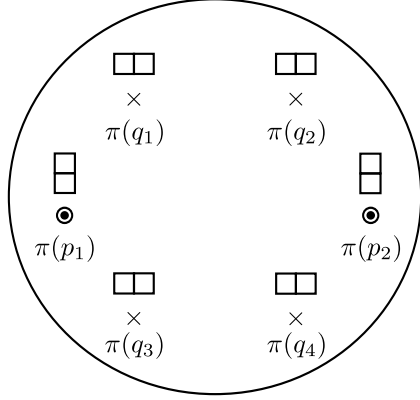


Figure 23: C_B for $SU(2)$ gauge theory with two massive hypermultiplets when the brane configuration is symmetric

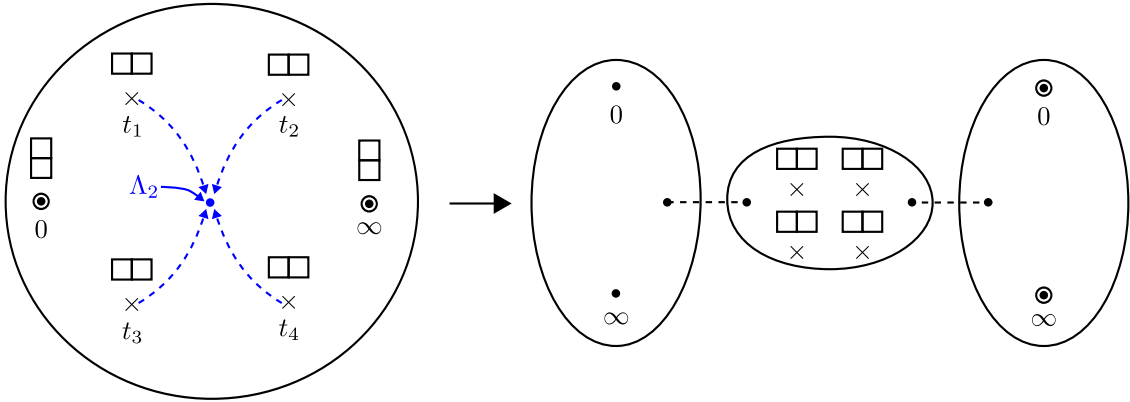


Figure 24: Behaviors of the new branch points when $m_1 = m_2 \rightarrow \Lambda_2$, $u_2 \rightarrow \Lambda_2^2$

the four branch points approach $t = \Lambda_2$. Figure 24 illustrates the behavior of the branch points under the limits. This is a similar situation of four branch points of index 2 gathering together around a point as we have seen in Sections 4 and 5. Imagine cutting off the region where the four points are together when we are in the vicinity of the limit. Going around the four points makes a complete journey, that is, we can come back to the branch of $v(t)$ where we started, which implies that adding a point of ramification index 1 to each branch of the excised region gives us a compact small torus. The two branches of the remaining part of the original Seiberg-Witten curve after the removal of the four branch points become two Riemann spheres after adding a point to each. This can also be seen by taking the Coulomb branch limit of the parameters in Eq. (6.2), which results in two components that have no ramification over t , that is, two Riemann spheres. Therefore we can identify a small torus and see nonlocal states becoming massless simultaneously as the cycles around the two of the four branch points vanish as we take the limits. It would be interesting to find out the

explicit expression for the small torus as we did in Section 5 where we found the algebraic equation that describes the small torus of Argyres-Douglas fixed points.

We have another brane configuration that gives us the same four-dimensional physics, which is shown in Figure 25. Now the D4-branes that provide massive hypermultiplets are on one side only, thereby losing the symmetry of flipping t to its inverse and swapping m_1 and m_2 .

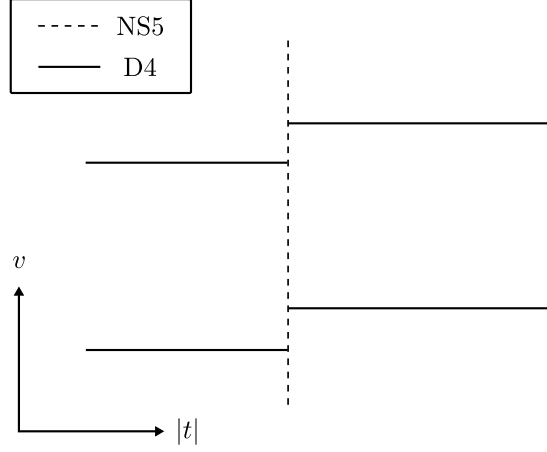


Figure 25: Brane configuration of $SU(2)$ gauge theory with two massive hypermultiplets, with asymmetric distribution of D4-branes

Corresponding Seiberg-Witten curve C_{SW} is given by the zero locus of

$$\tilde{f}(t, v) = \Lambda_2^2 t^2 - (v^2 - u_2)t + (v - m_1)(v - m_2). \quad (6.4)$$

After the usual analysis, we can find C_B and its branch points as shown in Figure 26.

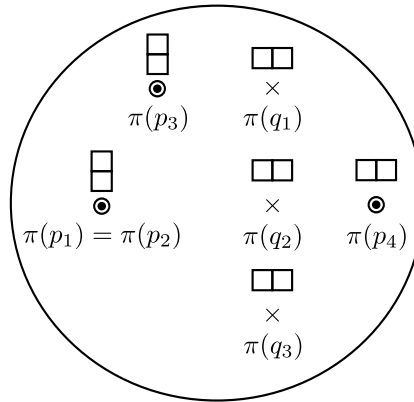


Figure 26: C_B for $SU(2)$ gauge theory with two massive hypermultiplets when the brane configuration is not symmetric

Here p_i 's are the points on \mathcal{C}_{SW} such that

$$\sigma(p_1) = (0, m_1), \sigma(p_2) = (0, m_2), \sigma(p_3) = (1, \infty), \sigma(p_4) = (\infty, \infty),$$

are the points we add to \mathcal{C}_{SW} to compactify it. Note that two of the images of p_i 's under π , $t = 0$ and $t = 1$, are not branch points in this case, because each of them has a trivial ramification there as indicated with the corresponding Young tableau. $t = \infty$ is a branch point. The locations of the other three branch points $\{\pi(q_i)\}$ are given as the three roots $\{t_i\}$ of Eq. (6.5).

$$\Lambda_2^2 t^3 + (u_2 - \Lambda_2^2) t^2 + (m_1 m_2 - u_2) t + \left(\frac{m_1 - m_2}{2}\right)^2 = 0. \quad (6.5)$$

Again we see that the locations of the branch points depend on the mass parameters as well as the Coulomb branch parameters and the scale.

From Eq. (6.5), we can easily identify the limits of the parameters that send $\pi(q_i)$'s to $t = 0$. That is,

- (1) When $m_1 = m_2 = m$, $t_1 \rightarrow 0$.
- (2) When $m^2 = u_2$, t_1 and $t_2 \rightarrow 0$.
- (3) When $m = \Lambda_2^2$, t_1 , t_2 , and $t_3 \rightarrow 0$.

The case of (3) is illustrated in the left side of Figure 27. Note that when we take the limit

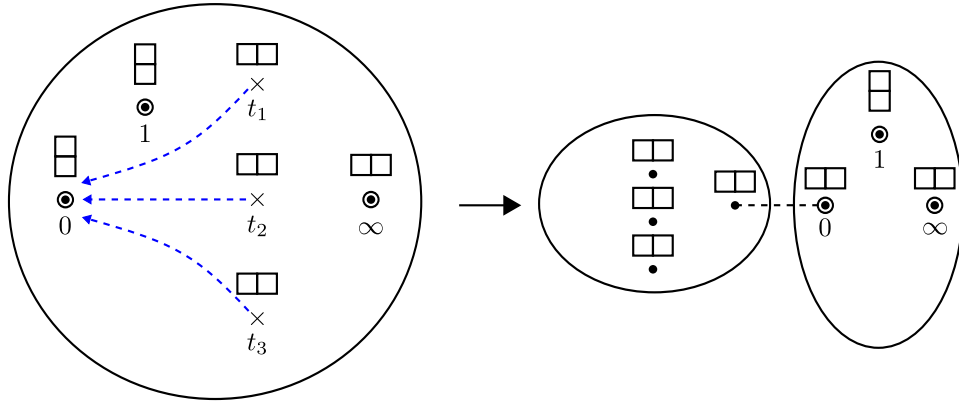


Figure 27: Behaviors of the new branch points when $m_1 = m_2 \rightarrow \Lambda_2$, $u_2 \rightarrow \Lambda_2^2$

$$m_1 = m_2 \rightarrow \Lambda_2, u_2 \rightarrow \Lambda_2^2,$$

the three branch points go to $t = 0$ and we can see that there are nonlocal states that become massless together in the limit. This is the same limit of the parameters as the one in the previous case of different brane configuration, a symmetric brane configuration. Therefore

we observe the phenomenon of seemingly different brane configurations giving the same four-dimensional physics.

However, unlike the previous case of symmetric brane configuration, where there are four branch points with ramification index 2 that are coming together under a specific limit, here there are only three of them moving toward a point. But note that while going around four branch points once gets us back to where we started, going around three branch points once does not complete a roundtrip but we need one more trip to get back to the starting point. This implies that, when excising the region that the three branch points come together, we need to add a point with ramification index 2 to both the excised part and the remaining part of the Seiberg-Witten curve. Then we have one curve with four branch points with ramification index 2, which is the small torus, and the other curve with two branch points with ramification index 2, which is a Riemann sphere. This procedure is illustrated in the right side of Figure 27. This can also be seen by taking the Coulomb branch limit of the parameters of Eq. (6.4), which gives us a curve with two ramification points of index 2, the Riemann sphere.

7. Discussion and outlook

Here we illustrated, through several examples, that when a Seiberg-Witten curve \mathcal{C}_{SW} of an $\mathcal{N} = 2$ gauge theory has a ramification over a Riemann sphere C_B , some of the branch points on C_B can be identified with the punctures of [4] but in general there are new branch points whose locations on C_B depend on various parameters of the theory and therefore can be a useful tool when studying various limits of the parameters, including Argyres-Seiberg duality and the Argyres-Douglas fixed points. Note that interesting phenomena happen when the branch points collide with each other. This is because those cases are exactly when the corresponding Seiberg-Witten curve becomes singular. The merit of utilizing the new branch points compared to the direct study of Seiberg-Witten curves is that it becomes more evident and easier to analyze when and how those limits of the parameters occur, as Gaiotto used his punctures and their collisions to investigate various corners of the moduli space of gauge coupling parameters.

Branch points have played a major role since the inception of the Seiberg-Witten curve. What is different here is that we can change the point of view such that we can find ramification points and their branch points in a way that is compatible with the setup of [4] so that we can complement and utilize the results from it. This change of the perspective can be illustrated as shown in Figure 28, which shows a brane configuration of $SU(3)$ theory with no matter. If we want to project the whole Seiberg-Witten curve onto a complex plane, there are two ways: one is projecting it onto the t -plane, and the other is projecting onto the v -plane. Prior to [4], the analysis of a Seiberg-Witten curve has been done by projecting the curve onto the v -plane so that it can be seen as a branched two-sheeted cover over the complex plane. Then the branch points are such that the corresponding ramification points on the Seiberg-Witten curve have the same ramification index of 2, because it is either 2 or

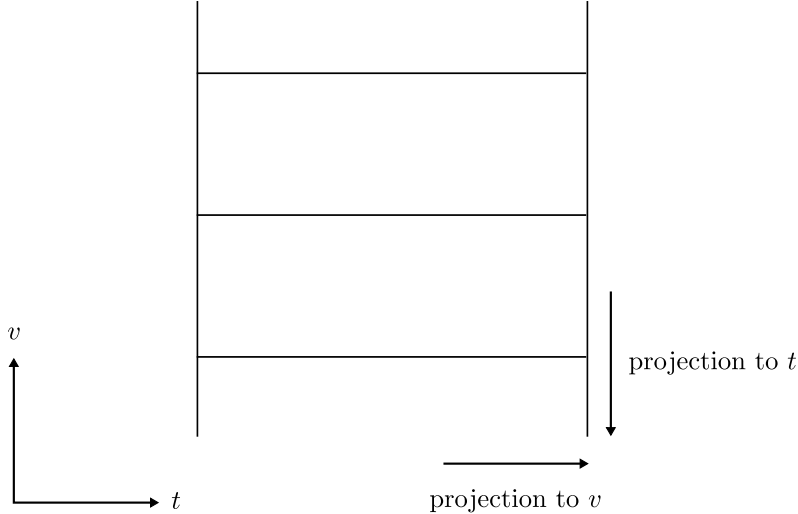


Figure 28: Two different ways of projecting a Seiberg-Witten curve onto a complex plane

1 for a two-sheeted covering map. But here we project the Seiberg-Witten curve onto the t -plane such that the curve is a three-sheeted cover over the complex plane.

This way of projecting a Seiberg-Witten curve makes it easier to understand the physical meaning of the branch points. When considering a Seiberg-Witten curve as a two-dimensional subspace of an M5-brane, Gaiotto told us that the curve can be described as several M5-branes wrapping a Riemann surface. Then a puncture corresponds to an M5-brane meeting several coincident M5-branes transversally. See Figure 29a which illustrates this configuration of M5-branes and their projection onto C_B . From the viewpoint of the coincident M5-branes, the other M5-brane is heavy and therefore can be considered as an operator when studying the theory living on the coincident M5-branes.

In comparison to that, a new branch point that we have studied here and is not related to a puncture comes from a ramification point of an M5-brane, which was the coincident M5-branes before turning on the Coulomb branch parameters of the theory. Nonzero Coulomb branch parameters make them move away from each other, and the result is one smooth but ramified M5-brane whose two-dimensional subspace is interpreted as a Seiberg-Witten curve of the theory. Figure 29b illustrates an M5-brane with two ramification points and their projection onto C_B . Again considering the whole curve as from several sheets of M5-branes, a ramification point is where those M5-branes come into a contact. It would be interesting if we can investigate the local physics around these points.

Formulating a cookbook-style procedure of constructing our C_B not from the analysis starting from the equation of a Seiberg-Witten curve but from the punctured Riemann surface of [4] with topological constraints, Coulomb branch parameters, and mass parameters would be interesting. Finding out how many of them are there and what ramification index each of them has will not be a difficult job. For example, when a Seiberg-Witten curve has genus 1

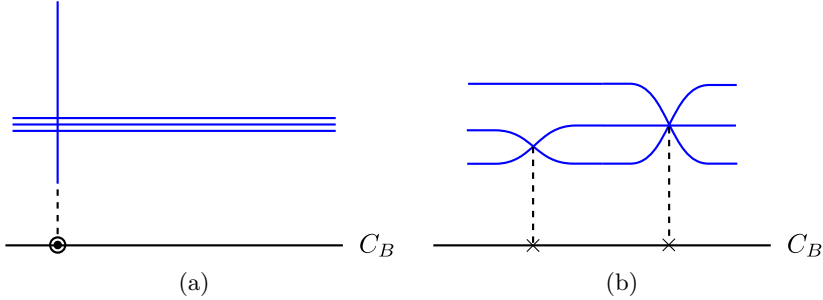


Figure 29: Configuration of M5-branes (a) near a puncture and (b) around ramification points

and if we know how many points of nontrivial ramification index we have to add to C_{SW} to compactify it, say n of them, then there should be $(4 - n)$ additional branch points on C_B because the Riemann-Hurwitz formula requires C_B to have four branch points in this case. We can do a similar job for the other cases. What is difficult is to figure out the dependence of the locations of the branch points on various parameters of the Seiberg-Witten curve, including gauge coupling parameters, Coulomb branch parameters, and mass parameters. If there is a way to see the dependence without the long and tedious analysis we presented here, it will be helpful for pursuing many interesting limits of the parameters.

As we have focused only on the local description near each branch point, there is an ambiguity of how to patch the local descriptions into a global one, because branches can be permuted by the monodromy of the parameters. It would be helpful if we can clear up that ambiguity explicitly.

Acknowledgments

It is a great pleasure to express sincere thanks to Sergei Gukov who provided precious advice at the various stages of the development of this work, and to John H. Schwarz for enlightening discussions at the finalizing stage of this work, careful reading of this manuscript, and generous support in many ways. The author also thanks Heejoong Chung, Petr Hořava, Christoph Keller, Sangmin Lee, Sungjay Lee, Yu Nakayama, Jaewon Song, and Piotr Sułkowski for helpful discussions. The author is grateful to the organizers of the 8th Simons Workshop in Mathematics and Physics at the Stony Brook University, where part of this work was completed, for their great hospitality. This work is supported in part by a Samsung Scholarship.

A. Normalization of singular algebraic curves

To understand how normalization works, let's try to normalize a curve with a singularity, $\bar{A} \subset \mathbb{CP}^2$, shown in the lower left side of Figure 30. The figure illustrates how a singularity of \bar{A} is resolved when we normalize it to a smooth curve $\mathcal{A} = \sigma^{-1}(\bar{A})$ by finding a map σ .

There are various kinds of singular points. The case illustrated in Figure 30 is that \bar{A} has a singular point $\sigma(s_1) = \sigma(s_2)$ which corresponds to two different points $\sigma^{-1}(s_1) = \{s_1, s_2\}$

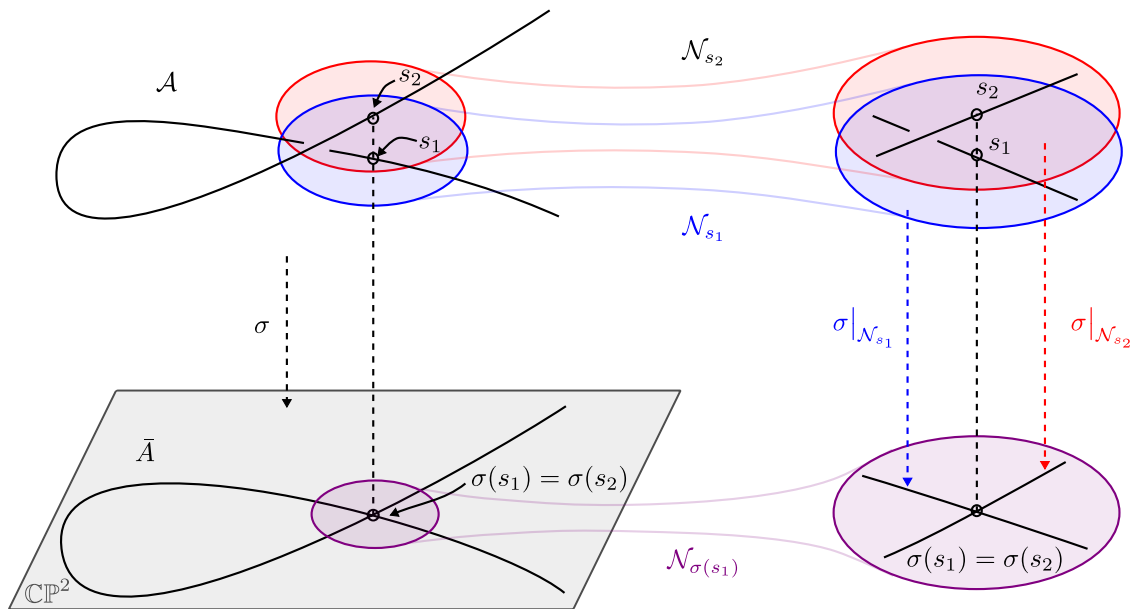


Figure 30: Schematic description of the (local) normalization of a singular curve

on \mathcal{A} . A similar kind of singularity occurs at $(z, w) = (0, 0)$ of a curve defined by $zw = 0$ in \mathbb{C}^2 . The singularity can be lifted if we consider embedding the curve into \mathbb{C}^3 and moving $z = 0$ and $w = 0$ complex planes away from each other along the other complex dimension normal to both of them.

Finding such σ that works over all $\bar{\mathcal{A}}$ will not be an easy job, especially because we don't know how to describe \mathcal{A} globally. However if we are interested only in analyzing a local neighborhood of a point on $\bar{\mathcal{A}}$, we do not need to find σ that maps the whole \mathcal{A} to the entire $\bar{\mathcal{A}}$, but finding a local normalization [9, 8] of $\bar{\mathcal{A}}$ near the point will be good enough for that purpose. What is good about this local version of normalization is that we know how to describe \mathcal{A} locally, because it is a Riemann surface. More precisely, a local normalization is a map $\sigma|_{\mathcal{N}_{s_0}}$ from the neighborhood of a point $s_0 \in \mathcal{A}$ to the neighborhood of $\sigma(s_0) \in \bar{\mathcal{A}}$.

$$\sigma|_{\mathcal{N}_{s_0}} : \mathcal{N}_{s_0} \rightarrow \mathcal{N}_{\sigma(s_0)}, \quad s \mapsto [X(s), Y(s), Z(s)].$$

Because \mathcal{A} is a Riemann surface we can choose a coordinate $s \in \mathbb{C}$ on \mathcal{A} such that $s_0 = 0$.

Now let's get back to the case of Figure 30 and find its local normalizations. Schematic descriptions of the local normalizations are shown in the right side of Figure 30, where the point of our interest, $\sigma(s_1)$, is a singular point of $\bar{\mathcal{A}}$. Without any normalization, $\bar{\mathcal{A}}$ is an irreducible curve that is singular at $\sigma(s_1)$. After a global normalization, we get a smooth irreducible curve \mathcal{A} . However, when we zoom into the neighborhood $\mathcal{N}_{\sigma(s_1)}$ of a singular point $\sigma(s_1)$ on $\bar{\mathcal{A}}$, we see a reducible curve with two irreducible components, each of which is a part of \mathcal{A} when considering the global normalization and is called a local analytic curve

[8]. By choosing $\mathcal{N}_{\sigma(s_1)}$ as small as possible, we can get a good approximation of the local analytic curves by finding a Puiseux expansion [7] of \bar{A} at $\sigma(s_1)$. By factorizing the Puiseux expansion into the irreducible components, we can get a good local picture of \mathcal{A} given by $\sigma|_{\mathcal{N}_{s_i}}$ for each component.

In the main text and in the following sections we have denoted a local normalization by the same symbol as its global version, omitting the neighborhood we are restricting the global normalization to and understanding it is valid only in the neighborhood. In principle we can sew up the local normalizations to get a global normalization if we have enough of them to cover the whole curve.

B. Compactification of a Seiberg-Witten curve

Let's consider how to compactify the Seiberg-Witten curve of $SU(2)$ SCFT as an example. The Seiberg-Witten curve C_{SW} of this theory is described by the zero locus of

$$f(t, v) = (t - 1)(t - t_1)v^2 - ut, \quad (\text{B.1})$$

which is a smooth, non-compact Riemann surface. The following four points

$$(t, v) = (0, 0), (1, \infty), (t_1, \infty), (\infty, 0),$$

are not included in C_{SW} .

Now let's compactify C_{SW} by embedding it into \mathbb{CP}^2 as a curve defined as the zero locus of

$$F(X, Y, Z) = (X - Z)(X - t_1Z)Y^2 - uXZ^3,$$

which we will call \bar{C}_{SW} . The four points $(t, v) = (0, 0), (1, \infty), (t_1, \infty), (\infty, 0) \in \mathbb{C}^2$ are now mapped to

$$[X, Y, Z] = [0, 0, 1], [0, 1, 0], [0, 1, 0], [1, 0, 0] \in \mathbb{CP}^2$$

respectively. But this compactification introduces singularities, as \bar{C}_{SW} is singular at

$$\{[X, Y, Z] = [0, 1, 0], [1, 0, 0]\},$$

which implies that \bar{C}_{SW} is not a Riemann surface. The singularity at $[0, 1, 0]$ corresponds to having two different tangent, the case we illustrated in Appendix A. The other singularity, $[1, 0, 0]$, corresponds to a cusp. These singularities can be resolved by the previously described procedure of normalization, after which we can find, for every point $s_0 \in C_{SW}$, the local normalization map

$$\sigma : C_{SW} \rightarrow \bar{C}_{SW}, s \mapsto [X(s), Y(s), Z(s)],$$

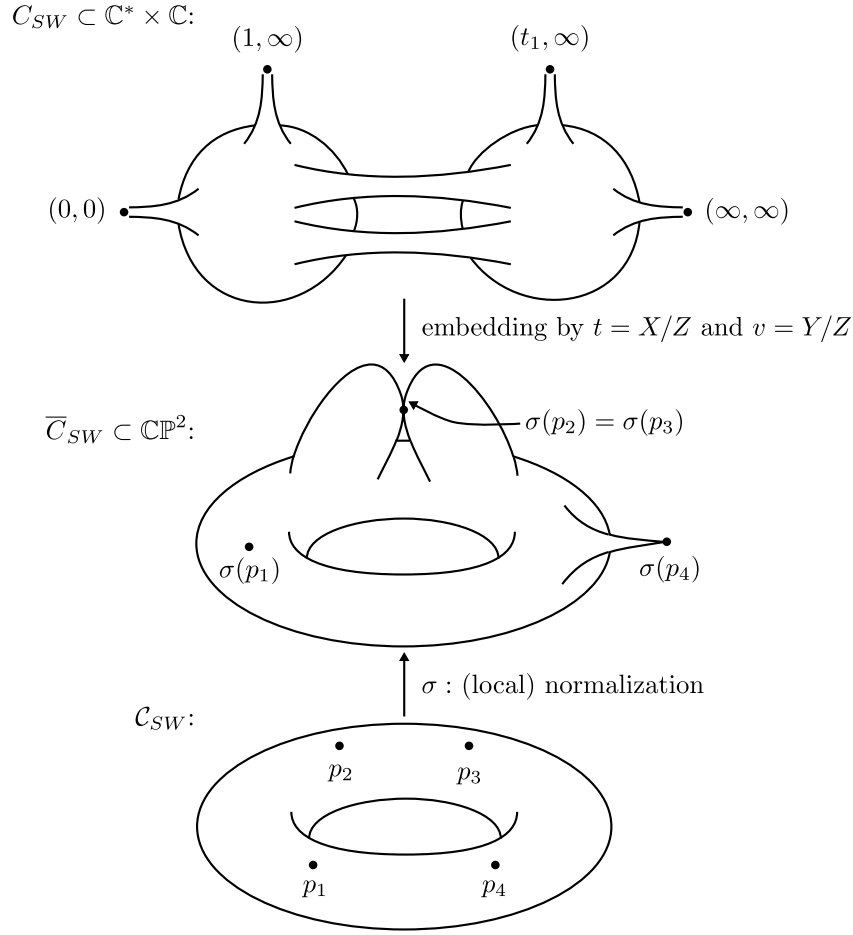


Figure 31: Schematic description of the compactification and the normalization of a Seiberg-Witten curve

where $s \in \mathbb{C}$ is a local coordinate such that $s_0 = 0$. Figure 31 illustrates the compactification and the normalization.

Using this local normalization map, we define $\pi : \mathcal{C}_{SW} \rightarrow \mathbb{CP}^1$ as

$$\pi(s) = t(s) = \frac{X(s)}{Z(s)},$$

where $t(s)$ has the value of the t -coordinate of

$$\mathcal{C}_{SW} \cup \{(t, v) \mid (0, 0), (1, \infty), (t_1, \infty), (\infty, 0)\},$$

and therefore has the range of

$$\mathbb{C}^* \cup \{0\} \cup \{\infty\} = \mathbb{CP}^1.$$

Note that $t(s)$ is well-defined over \mathcal{C}_{SW} , although $X/Z : \bar{\mathcal{C}}_{SW} \rightarrow \mathbb{CP}^1$ is not well-defined at $[0, 1, 0] \in \bar{\mathcal{C}}_{SW}$ because it can have two different values there, 1 and t_1 . This ill-definedness arises because we compactify \mathcal{C}_{SW} by embedding it into \mathbb{CP}^2 , which maps two different points on \mathcal{C}_{SW} , $(1, \infty)$ and (t_1, ∞) , to one point in \mathbb{CP}^2 , $[0, 1, 0]$, and therefore is the artifact of our embedding scheme. Normalization separates the two local analytic curve that meet at $[0, 1, 0]$ and resolves this difficulty, after which $t(s)$ is a well-defined function over the two local analytic curves and therefore over all \mathcal{C}_{SW} . This π gives us the ramification of \mathcal{C}_{SW} over \mathbb{CP}^1 that we want.

After embedding \mathcal{C}_{SW} into \mathbb{CP}^2 , the Seiberg-Witten differential form $\lambda = \frac{v}{t} dt$, which is a meromorphic 1-form on \mathcal{C}_{SW} , becomes⁵

$$\lambda = \frac{Y}{X} d\left(\frac{X}{Z}\right)$$

and it defines a meromorphic 1-form on $\bar{\mathcal{C}}_{SW}$. Therefore $\omega = \sigma^*(\lambda)$ defines a meromorphic 1-form on \mathcal{C}_{SW} .

C. Calculation of local normalizations

Calculation of a local normalization of a curve near a point is done here by finding a Puiseux expansion [7] of the curve at the point. Puiseux expansion is essentially a convenient way to get a good approximation of a curve in \mathbb{CP}^2 around a fixed point.

C.1 $SU(2)$ SCFT

We showed in Appendix B how to compactify the Seiberg-Witten curve of $SU(2)$ SCFT. So let's start with the compactified curve, $\bar{\mathcal{C}}_{SW}$, that is defined as the zero locus of

$$F(X, Y, Z) = (X - Z)(X - t_1 Z)Y^2 - uXZ^3$$

in \mathbb{CP}^2 . We want to get the local normalizations near

- (1) $\{p_i \in \mathcal{C}_{SW}\}$, where $\sigma(p_i)$'s are the points we added to compactify \mathcal{C}_{SW} ,
- (2) $\{q_i \in \mathcal{C}_{SW} | dt(q_i) = 0\} \Leftrightarrow \{q_i \in \mathcal{C}_{SW} | (\partial f / \partial v)(t(q_i), v(q_i)) = 0\}$,
- (3) $\{r_i \in \mathcal{C}_{SW} | v(r_i) = 0\}$.

The corresponding points on $\bar{\mathcal{C}}_{SW}$ are

$$\begin{aligned} \sigma(p_1) &= [0, 0, 1], \\ \sigma(p_2) &= \sigma(p_3) = [0, 1, 0], \\ \sigma(p_4) &= [1, 0, 0], \end{aligned}$$

from (1). (2) and (3) does not give any new candidates.

⁵Whether this embedding of λ is justifiable is a part of the question that the embedding of \mathcal{C}_{SW} into \mathbb{CP}^2 gives the same physics as \mathcal{C}_{SW} does or not.

1. Near $\sigma(p_1) = [0, 0, 1]$, let's denote a small deviation from $[0, 0, 1]$ by $[x, y, 1]$. Along \bar{C}_{SW} x and y satisfy

$$F(x, y, 1) = (x - 1)(x - t_1)y^2 - ux = 0. \quad (\text{C.1})$$

From this polynomial we can get the corresponding Newton polygon. Here is how we get one. First we mark a point at $(a, b) \in \mathbb{Z}^2$ if we have in the polynomial a term $x^a y^b$ with nonzero coefficient. We do this for every term in the polynomial and get several points in the \mathbb{Z}^2 -plane. For instance, the polynomial (C.1) gives the points in Figure 32, where the horizontal axis corresponds to the exponent of x and the vertical one to that of y for a term that is represented as a point. Now we connect some of the points with

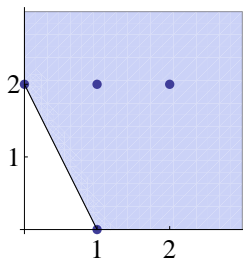


Figure 32: Newton polygon of $F(x, y, 1)$

lines so that the lines with the two axes make a polygon that contains all the points and is convex to the origin. This is the Newton polygon of the polynomial.

Using this Newton polygon, we can find a Puiseux expansion at $\sigma(p_1)$. The underlying principle why it works is illustrated in [7], for example. Here we will describe just how we can get the Puiseux expansion using the data we have at hand. First we pick a line segment that corresponds to the steepest slope and collect the terms corresponding to the points on that edge to make a new polynomial. Then the zero locus of the polynomial is the local representation of \bar{C}_{SW} near $[0, 0, 1]$. In this case, the new polynomial is

$$t_1 y^2 - ux.$$

This is the lowest-order approximation of \bar{C}_{SW} at $x = y = 0$. We can get a better approximation by including “higher-order” terms, but this is enough for now. If we represent the zero locus of this polynomial as

$$y(x) = \pm \sqrt{\frac{ux}{t_1}},$$

this is the Puiseux expansion of y in x at $x = y = 0$. We can see that there are two branches of $y(x)$ and that the two branches are coming together at $x = y = 0$.

To get a local normalization near the point, note that

$$\sigma : s \mapsto [x, y, 1] = [s^2, a_0 s, 1], \quad a_0 = \sqrt{u/t_1}$$

maps a neighborhood of $s = 0$ to the two branches. Therefore σ is a good local normalization when we consider s as a coordinate patch for \mathcal{C}_{SW} where p_1 is located at $s = 0$.

Now we have a local normalization σ near p_1 . Let's use this to calculate the ramification index $\nu_{p_1}(\pi)$. Remember that $\pi : \mathcal{C}_{SW} \rightarrow C_B$ is realized in Section 2 as

$$\pi : \mathcal{C}_{SW} \rightarrow \mathbb{CP}^1, s \mapsto \frac{X(s)}{Z(s)}.$$

Near $s = 0$,

$$\pi(s) - \pi(p_1) = \frac{x(s)}{1} - 0 = s^2.$$

The exponent of this map is the ramification index at $s = 0$. That is, $\nu_{p_1}(\pi) = 2$.

We can also calculate the degree of (ω) at p_1 using the local normalization. Remember that (ω) is the Seiberg-Witten differential pulled back by σ onto \mathcal{C}_{SW} .

$$\omega = \sigma^*(\lambda) = \sigma^* \left(\frac{Y/Z}{X/Z} d \left(\frac{X}{Z} \right) \right).$$

Near $s = 0$, this becomes

$$\omega = \frac{y(s)}{x(s)} d(x(s)) = \frac{a_0 s}{s^2} \cdot d(s^2) = 2a_0 ds.$$

Therefore ω has neither pole nor zero of any order at $s = 0$, which implies $\nu_{p_1}(\omega) = 0$.

2. Near $\sigma(p_2) = \sigma(p_3) = [0, 1, 0]$, let's denote a deviation from $[0, 1, 0]$ by $[x, 1, z]$. Then along \bar{C}_{SW} x and z satisfy

$$F(x, 1, z) = (x - z)(x - t_1 z) - uxz^3 = 0.$$

The Newton polygon of this polynomial is shown in Figure 33. We collect the terms

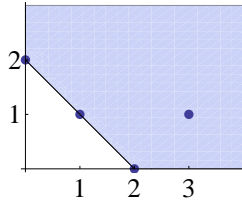


Figure 33: Newton polygon of $F(x, 1, z)$

corresponding to the points on the edge to get a polynomial, whose zero locus is the local representation of \bar{C}_{SW} near $[0, 1, 0]$.

$$x^2 + xz(-1 - t_1) + z^2 t_1 = (x - z)(x - t_1 z).$$

Note that this polynomial is reducible and has two irreducible components. This is the situation described in Figure 30. Therefore we can see that $[0, 1, 0]$ has two preimages p_2 and p_3 on \mathcal{C}_{SW} by σ . But this local representation is not accurate enough for us to calculate R_π or (ω) . To see this, let's focus on one of the two components, $x - t_1z$. This gives us the following local normalization near p_3 .

$$\sigma : s \mapsto [x, 1, z] = [t_1s, 1, s].$$

From this normalization we get

$$\pi(s) = \frac{x(s)}{z(s)} = t_1,$$

which maps the neighborhood of $s = 0$ on \mathcal{C}_{SW} to a point on C_B . Also,

$$\omega = \frac{1}{x(s)} d \left(\frac{x(s)}{z(s)} \right) = \frac{1}{t_1s} d(t_1) = 0,$$

which does not make sense. The reason for these seemingly inconsistent results is because the approximation we have is not accurate enough to capture the true nature of $\bar{\mathcal{C}}_{SW}$. Therefore we need to include “higher-order” terms of the Puiseux expansion. To do this we first pick one of the two components that we want to improve our approximation. Let's stick with $x - t_1z$. The idea is to get a better approximation by including more terms of higher order. That is, we add to

$$x(z) = t_1z$$

one more term

$$x(z) = z(t_1 + x_1(z))$$

and then find such $x_1(z)$. For that purpose we put the relation back into $F(x, 1, z)$. Then we get

$$F(z(t_1 + x_1), 1, z) = z^2 F_1(x_1, z),$$

where we factored out z^2 that is the common factor of every term in F . Now we draw the Newton polygon of F_1 and do the same job as we have done so far. The Newton polygon is shown in Figure 34. Collecting the terms on the line segment gives

$$(t_1 - 1)x_1 - ut_1z^2.$$

Setting this to zero gives $x_1(z)$, and by putting it back to $x(z)$, we get

$$x = z(t_1 + x_1(z)) = t_1z + \frac{t_1u}{t_1 - 1}z^3.$$

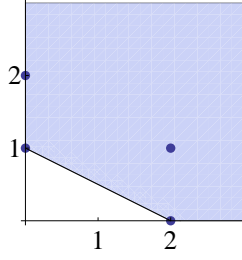


Figure 34: Newton polygon of $F_1(x_1, z)$

We now have a better approximation to \bar{C}_{SW} . If we want to do even better, we can iterate this process. But, as we will see below, this is enough for us for now, so we will stop here.

For the other irreducible component, $x - z$, we do a similar calculation and get the same Newton polygon and the following Puiseux expansion.

$$x = z(1 + x_1(z)) = z + \frac{u}{1 - t_1} z^3.$$

These expansions give us the following local normalizations

$$\sigma : s \mapsto [x, 1, z] = [b_0 s + b_1 s^3, 1, s],$$

where b_0 and b_1 are

$$b_0 = 1, \quad b_1 = \frac{u}{1 - t_1}$$

at p_2 and

$$b_0 = t_1, \quad b_1 = \frac{t_1 u}{t_1 - 1}$$

at p_3 . From each of these local normalizations we get, near $s = 0$,

$$\pi(s) - \pi(p_i) = \frac{x(s)}{z(s)} - b_0 \propto s^2 \Rightarrow \nu_{p_2}(\pi) = \nu_{p_3}(\pi) = 2,$$

and

$$\omega = \frac{1}{x(s)} d \left(\frac{x(s)}{z(s)} \right) \propto ds \Rightarrow \nu_{p_2}(\omega) = \nu_{p_3}(\omega) = 0.$$

3. Next, consider $\sigma(p_4) = [1, 0, 0]$. We start by denoting the deviations from $[1, 0, 0]$ as $[1, y, z]$. Then y and z satisfy

$$F(1, y, z) = (1 - z)(1 - t_1 z)y^2 - uz^3 = 0,$$

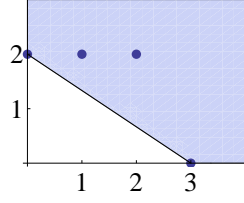


Figure 35: Newton polygon of $F(1, y, z)$

whose Newton polygon is shown in Figure 35. This gives us a polynomial

$$y^2 - uz^3,$$

which is a local representation of \tilde{C}_{SW} near $y = z = 0$. The corresponding local normalization is

$$\sigma : s \mapsto [1, y, z] = [1, c_0 s^3, s^2], \quad c_0 = \sqrt{u}.$$

Using this local normalization, we get

$$\frac{1}{\pi(s)} - \frac{1}{\pi(p_4)} = \frac{z(s)}{1} - \frac{1}{\infty} \propto s^2 \Rightarrow \nu_{p_4}(\pi) = 2,$$

where we took a reciprocal of $\pi(s)$ because $\pi(s=0) = \pi(p_4) = \infty$. And we also find

$$\omega = y(s)d\left(\frac{1}{z(s)}\right) \propto ds \Rightarrow \nu_{p_4}(\omega) = 0.$$

As we have found out in Sections 2, for the example of this section p_1, p_2, p_3 , and p_4 are all of the points that we need to investigate. Therefore we have all the local normalizations we need to construct R_π and ω . From the results of this subsection, we have

$$R_\pi = 1 \cdot [p_1] + 1 \cdot [p_2] + 1 \cdot [p_3] + 1 \cdot [p_4]$$

and

$$(\omega) = 0.$$

C.2 $SU(2) \times SU(2)$ SCFT

The corresponding Seiberg-Witten curve C_{SW} is the zero locus of

$$f(t, v) = (t-1)(t-t_1)(t-t_2)v^2 - u_1 t^2 - u_2 t. \quad (\text{C.2})$$

We embed this into \mathbb{CP}^2 and add to it $\{[X, Y, Z] = [0, 0, 1], [0, 1, 0], [1, 0, 0]\}$ to compactify it to \tilde{C}_{SW} , the zero locus of

$$F(X, Y, Z) = (X-Z)(X-t_1 Z)(X-t_2 Z)Y^2 - u_1 X^2 Z^3 - u_2 X Z^4.$$

in \mathbb{CP}^2 . Now we want to get the local normalizations near

- (1) $\{p_i \in \mathcal{C}_{SW}\}$, where $\sigma(p_i)$'s are the points we added to compactify \mathcal{C}_{SW} ,
- (2) $\{q_i \in \mathcal{C}_{SW} | dt(q_i) = 0\} \Leftrightarrow \{q_i \in \mathcal{C}_{SW} | (\partial f / \partial v)(t(q_i), v(q_i)) = 0\}$,
- (3) $\{r_i \in \mathcal{C}_{SW} | v(r_i) = 0\}$.

The corresponding points on $\bar{\mathcal{C}}_{SW}$ are

$$\begin{aligned}\sigma(p_1) &= [0, 0, 1], \\ \sigma(p_2) = \sigma(p_3) = \sigma(p_4) &= [0, 1, 0], \\ \sigma(p_5) &= [1, 0, 0],\end{aligned}$$

from (1), and

$$\sigma(q) = [\rho, 0, 1], \quad \rho = -u_2/u_1$$

from (2). (3) does not give any new candidates.

1. Near $\sigma(p_1) = [0, 0, 1]$, the Newton polygon of $F(x, y, 1)$ is shown in Figure 36. This

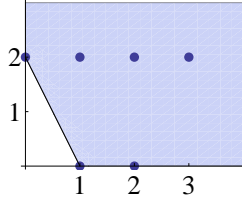


Figure 36: Newton polygon of $F(x, y, 1)$

gives us a polynomial

$$t_1 t_2 y^2 + u_2 x,$$

whose zero locus is the local representation of $\bar{\mathcal{C}}_{SW}$ at $x = y = 0$. The local normalization near p_1 is

$$\sigma : s \mapsto [x, y, 1] = [s^2, a_0 s, 1], \quad a_0 = \sqrt{-u_2 / (t_1 t_2)},$$

from which we can get

$$\begin{aligned}\pi(s) - \pi(p_1) &= \frac{x(s)}{1} - 0 \propto s^2 \Rightarrow \nu_{p_1}(\pi) = 2, \\ \omega &= \frac{y(s)}{x(s)} d(x(s)) \propto ds \quad \Rightarrow \nu_{p_1}(\omega) = 0.\end{aligned}$$

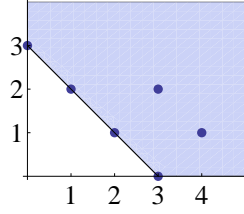


Figure 37: Newton polygon of $F(x, 1, z)$

2. Near $\sigma(p_2) = \sigma(p_3) = \sigma(p_4) = [0, 1, 0]$, the Newton polygon of $F(x, 1, z)$ is shown in Figure 37. This gives us

$$x^3 + x^2z(-1 - t_1 - t_2) - z^3t_1t_2 + xz^2(t_1 + t_2 + t_1t_2) = (x - z)(x - t_1z)(x - t_2z),$$

whose zero locus is the local representation of \bar{C}_{SW} at $x = z = 0$. We see that it has three irreducible components, and that each component needs a higher-order term to calculate $\nu_{p_i}(\pi)$ and $\nu_{p_i}(\omega)$. We pick a component

$$x = b_0z.$$

By denoting the higher-order term as $x_1(z)$, now $x(z)$ is

$$x = z(b_0 + x_1(z)), \quad b_0 = \begin{cases} 1 & \text{at } p_2, \\ t_1 & \text{at } p_3, \\ t_2 & \text{at } p_4. \end{cases}$$

and by putting this back into $F(x, 1, z)$, we get

$$F(x, 1, z) = z^3F_1(x_1, z).$$

The Newton polygon of $F_1(x_1, z)$ is shown in Figure 38. This gives us a polynomial

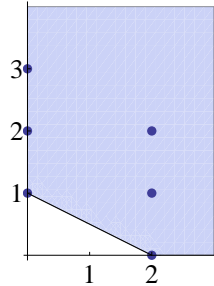


Figure 38: Newton polygon of $F_1(x_1, z)$

$$x_1 - b_1 z^2, b_1 = \begin{cases} \frac{u_1+u_2}{(1-t_1)(1-t_2)} & \text{at } p_2, \\ \frac{t_1(t_1 u_1+u_2)}{(t_1-1)(t_1-t_2)} & \text{at } p_3, \\ \frac{t_2(t_2 u_1+u_2)}{(t_2-1)(t_2-t_1)} & \text{at } p_4. \end{cases}$$

Therefore the Puiseux expansion at each p_i is

$$x = z(b_0 + x_1(z)) = b_0 z + b_1 z^3.$$

The local normalization near each p_i is

$$\sigma : s \mapsto [x, 1, z] = [b_0 s + b_1 s^3, 1, s],$$

from which we can get

$$\begin{aligned} \pi(s) - \pi(p_i) &= \frac{x(s)}{z(s)} - b_0 \propto s^2 \Rightarrow \nu_{p_i}(\pi) = 2, \\ \omega &= \frac{1}{x(s)} d \left(\frac{x(s)}{z(s)} \right) \propto ds \quad \Rightarrow \nu_{p_i}(\omega) = 0. \end{aligned}$$

3. Near $\sigma(p_5) = [1, 0, 0]$, the Newton polygon of $F(1, y, z)$ is shown in Figure 39. This

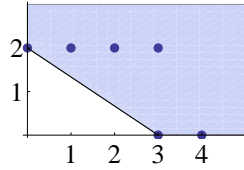


Figure 39: Newton polygon of $F(1, y, z)$

gives us

$$y^2 - u_1 z^3$$

as the local representation of \bar{C}_{SW} at $y = z = 0$. The local normalization near p_5 is

$$\sigma : s \mapsto [1, y, z] = [1, c_0 s^3, s^2], \quad c_0 = \sqrt{u_1},$$

from which we can get

$$\begin{aligned} \frac{1}{\pi(s)} - \frac{1}{\pi(p_4)} &= \frac{z(s)}{1} - \frac{1}{\infty} \propto s^2 \Rightarrow \nu_{p_5}(\pi) = 2, \\ \omega &= y(s) d \left(\frac{1}{z(s)} \right) \propto ds \quad \Rightarrow \nu_{p_5}(\omega) = 0. \end{aligned}$$

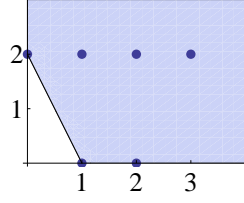


Figure 40: Newton polygon of $F(\rho + x, y, 1)$

4. Near $\sigma(q) = [\rho, 0, 1]$, the Newton polygon of $F(\rho + x, y, 1)$ is shown in Figure 40. This gives us a polynomial

$$u_2x - (\rho - 1)(\rho - t_1)(\rho - t_2)y^2,$$

whose zero locus is the local representation of \bar{C}_{SW} at $x = y = 0$. The local normalization near q is

$$\sigma : s \mapsto [\rho + x, y, 1] = [\rho + s^2, d_0s, 1], \quad d_0 = \sqrt{\frac{u_2}{(\rho - 1)(\rho - t_1)(\rho - t_2)}},$$

from which we can get

$$\begin{aligned} \pi(s) - \pi(q) &= \frac{\rho + x(s)}{1} - \rho \propto s^2 \Rightarrow \nu_q(\pi) = 2, \\ \omega &= \frac{d_0s}{\rho} d(x(s)) \propto s^2 ds \quad \Rightarrow \nu_q(\omega) = 2. \end{aligned}$$

From these results we can find out

$$\begin{aligned} R_\pi &= 1 \cdot [p_1] + 1 \cdot [p_2] + 1 \cdot [p_3] + 1 \cdot [p_4] + 1 \cdot [p_5] + 1 \cdot [q], \\ (\omega) &= 2 \cdot [q]. \end{aligned}$$

C.3 $SU(3)$ SCFT

The Seiberg-Witten curve C_{SW} is defined as the zero locus of

$$f(t, v) = (t - 1)(t - t_1)v^3 - u_2tv - u_3t$$

in $\mathbb{C}^* \times \mathbb{C}$. Now we embed C_{SW} into \mathbb{CP}^2 and add $\{[X, Y, Z] = [0, 0, 1], [0, 1, 0], [1, 0, 0]\}$ to compactify it to \bar{C}_{SW} , which is the zero locus of

$$F(X, Y, Z) = (X - Z)(X - t_1Z)Y^3 - u_2XYZ^3 - u_3XZ^4$$

in \mathbb{CP}^2 . We want to get the local normalizations near

- (1) $\{p_i \in C_{SW}\}$, where $\sigma(p_i)$'s are the points we added to compactify C_{SW} ,

$$(2) \{q_i \in \mathcal{C}_{SW} | dt(q_i) = 0\} \Leftrightarrow \{q_i \in \mathcal{C}_{SW} | (\partial f / \partial v)(t(q_i), v(q_i)) = 0\},$$

$$(3) \{r_i \in \mathcal{C}_{SW} | v(r_i) = 0\}.$$

(1) gives us

$$\begin{aligned} \sigma(p_1) &= [0, 0, 1], \\ \sigma(p_2) &= \sigma(p_3) = [0, 1, 0], \\ \sigma(p_4) &= [1, 0, 0], \end{aligned}$$

and (2) gives us

$$\sigma(q_{\pm}) = [t_{\pm}, v_0, 1].$$

(3) does not give any new candidate.

1. Near $\sigma(p_1) = [0, 0, 1]$, the Newton polygon of $F(x, y, 1)$ is shown in Figure 41. This

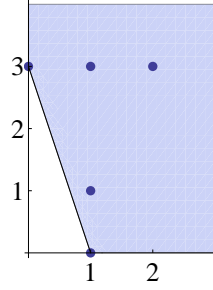


Figure 41: Newton polygon of $F(x, y, 1)$

gives us a polynomial

$$t_1 y^3 - u_3 x,$$

whose zero locus is the local representation of $\bar{\mathcal{C}}_{SW}$ at $x = y = 0$. The local normalization near p_1 is

$$\sigma : s \mapsto [x, y, 1] = [s^3, a_0 s, 1], \quad a_0 = \sqrt[3]{u_3/t_1},$$

from which we can get

$$\begin{aligned} \pi(s) - \pi(p_1) &= \frac{x(s)}{1} - 0 \propto s^3 \Rightarrow \nu_{p_1}(\pi) = 3, \\ \omega &= \frac{y(s)}{x(s)} d(x(s)) \propto ds \quad \Rightarrow \nu_{p_1}(\omega) = 0. \end{aligned}$$

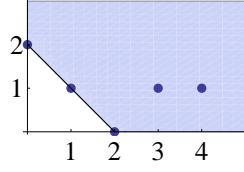


Figure 42: Newton polygon of $F(x, 1, z)$

2. Near $\sigma(p_2) = \sigma(p_3) = [0, 1, 0]$, the Newton polygon of $F(x, 1, z)$ is shown in Figure 42. This gives us

$$x^2 - (1 + t_1)xz + t_1z^2 = (x - z)(x - t_1z),$$

whose zero locus is the local representation of \bar{C}_{SW} at $x = z = 0$. We see that it has two irreducible components, and that each component needs a higher-order term to describe \bar{C}_{SW} up to the accuracy to calculate $\nu_{p_1}(\pi)$ and $\nu_{p_1}(\omega)$. We pick a component

$$x = b_0z, \quad b_0 = \begin{cases} 1 & \text{at } p_2, \\ t_1 & \text{at } p_3. \end{cases}$$

By denoting the higher-order term as $x_1(z)$, now $x(z)$ is

$$x = z(b_0 + x_1(z)),$$

and by putting this back into $F(x, 1, z)$, we get

$$F(x, 1, z) = z^2F_1(x_1, z).$$

The Newton polygon of $F_1(x_1, z)$ is shown in Figure 43. This gives us a polynomial

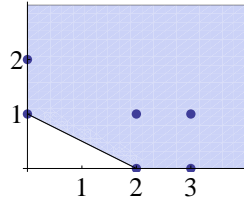


Figure 43: Newton polygon of $F_1(x_1, z)$

$$x_1 - b_1z^2, \quad b_1 = \begin{cases} \frac{u_2}{1-t_1} & \text{at } p_2, \\ \frac{t_1u_2}{t_1-1} & \text{at } p_3. \end{cases}$$

Therefore the Puiseux expansion at each p_i is

$$x = z(b_0 + x_1(z)) = b_0z + b_1z^3.$$

The local normalization near each p_i is

$$\sigma : s \mapsto [x, 1, z] = [b_0 s + b_1 s^3, 1, s],$$

from which we can get

$$\begin{aligned} \pi(s) - \pi(p_i) &= \frac{x(s)}{z(s)} - b_0 \propto s^2 \Rightarrow \nu_{p_i}(\pi) = 2, \\ \omega &= \frac{1}{x(s)} d \left(\frac{x(s)}{z(s)} \right) \propto ds \quad \Rightarrow \nu_{p_i}(\omega) = 0. \end{aligned}$$

3. Near $\sigma(p_4) = [1, 0, 0]$, the Newton polygon of $F(1, y, z)$ is shown in Figure 44. This

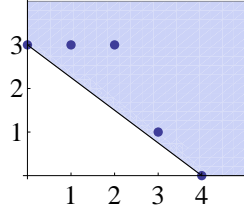


Figure 44

gives us

$$y^3 - u_3 z^4$$

as the local representation of \bar{C}_{SW} at $y = z = 0$. The local normalization near p_4 is

$$\sigma : s \mapsto [1, y, z] = [1, c_0 s^4, s^3], \quad c_0 = \sqrt[3]{u_3},$$

from which we can get

$$\begin{aligned} \frac{1}{\pi(s)} - \frac{1}{\pi(p_4)} &= \frac{z(s)}{1} - \frac{1}{\infty} \propto s^3 \Rightarrow \nu_{p_4}(\pi) = 3, \\ \omega &= y(s) d \left(\frac{1}{z(s)} \right) \propto ds \quad \Rightarrow \nu_{p_4}(\omega) = 0. \end{aligned}$$

4. Near $\sigma(q_{\pm}) = [t_{\pm}, v_0, 1]$, the Newton polygon of $F(t_{\pm} + x, v_0 + y, 1)$ is shown in Figure 45. This gives us a polynomial

$$\frac{1}{\rho} \left(\frac{1 + t_1 + \rho}{2} - t_{\pm} \right) x - \left(\frac{3t_{\pm}}{2v_0^2} \right) y^2, \quad \rho = \frac{(u_2/3)^3}{(u_3/2)^2},$$

whose zero locus is the local representation of \bar{C}_{SW} at $x = y = 0$. The local normalization near q_{\pm} is

$$\begin{aligned} \sigma : s \mapsto [t_{\pm} + x, v_0 + y, 1] &= [t_{\pm} + s^2, v_0 + d_0 s, 1], \\ d_0 &= v_0 \sqrt{\frac{2}{3\rho} \left(\frac{1 + t_1 + \rho}{2t_{\pm}} - 1 \right)}, \end{aligned}$$

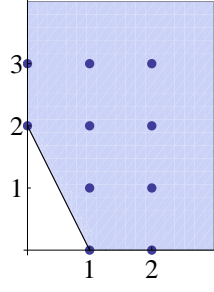


Figure 45: Newton polygon of $F(t_{\pm} + x, v_0 + y, 1)$

from which we can get

$$\begin{aligned} \pi(s) - \pi(q_{\pm}) &= \frac{t_{\pm} + x(s)}{1} - t_{\pm} \propto s^2 \Rightarrow \nu_{q_{\pm}}(\pi) = 2, \\ \omega &= \frac{v_0}{t_{\pm}} d(x(s)) \propto s ds \quad \Rightarrow \nu_{q_{\pm}}(\omega) = 1. \end{aligned}$$

From these results we get

$$\begin{aligned} R_{\pi} &= 2 \cdot [p_1] + 1 \cdot [p_2] + 1 \cdot [p_3] + 2 \cdot [p_4] + 1 \cdot [q_+] + 1 \cdot [q_-], \\ (\omega) &= 1 \cdot [q_+] + 1 \cdot [q_-]. \end{aligned}$$

C.4 $SU(3)$ pure gauge theory

The Seiberg-Witten curve C_{SW} is given by the zero locus of

$$f(t, v) = tv^3 - u_2tv + (t^2 - u_3t + 1).$$

We embed C_{SW} into \mathbb{CP}^2 and add $\{[X, Y, Z] = [0, 1, 0], [1, 0, 0]\}$ to it, which results in \bar{C}_{SW} , the zero locus of

$$F(X, Y, Z) = XY^3 - u_2XYZ^2 + (X^2Z^2 - u_3XZ^3 + Z^4).$$

in \mathbb{CP}^2 . We want to get the local normalizations near

- (1) $\{p_i \in C_{SW}\}$, where $\sigma(p_i)$'s are the points we added to compactify C_{SW} ,
- (2) $\{q_i \in C_{SW} | dt(q_i) = 0\} \Leftrightarrow \{q_i \in C_{SW} | (\partial f / \partial v)(t(q_i), v(q_i)) = 0\}$,
- (3) $\{r_i \in C_{SW} | v(r_i) = 0\}$.

(1) gives us

$$\begin{aligned} \sigma(p_1) &= [0, 1, 0], \\ \sigma(p_2) &= [1, 0, 0], \end{aligned}$$

(2) gives us

$$\sigma(q_{ab}) = [t_{2ab}, v_{2a}, 1],$$

and (3) gives us

$$\sigma(r_{\pm}) = [t_{3\pm}, 0, 1].$$

1. Near $\sigma(p_1) = [0, 1, 0]$, the Newton polygon of $F(x, 1, z)$ is shown in Figure 46. This

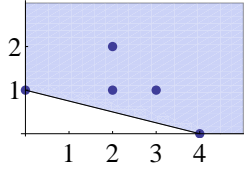


Figure 46: Newton polygon of $F(x, 1, z)$

gives us a polynomial

$$x + z^4,$$

whose zero locus is the local representation of \bar{C}_{SW} at $x = z = 0$. The local normalization near p_1 is

$$\sigma : s \mapsto [x, 1, z] = [-s^4, 1, s],$$

from which we can get

$$\begin{aligned} \pi(s) - \pi(p_1) &= \frac{x(s)}{z(s)} - 0 \propto s^3 \Rightarrow \nu_{p_1}(\pi) = 3, \\ \omega &= \frac{1}{x(s)} d \left(\frac{x(s)}{z(s)} \right) \propto \frac{ds}{s^2} \Rightarrow \nu_{p_1}(\omega) = -2. \end{aligned}$$

2. Near $p_2 = [1, 0, 0]$, the Newton polygon of $F(1, y, z)$ is shown in Figure 47. This gives

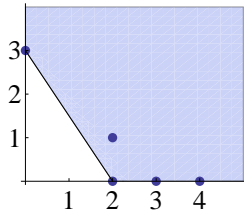


Figure 47: Newton polygon of $F(1, y, z)$

us

$$y^3 + z^2$$

as the local representation of \bar{C}_{SW} at $y = z = 0$. The local normalization near p_2 is

$$\sigma : s \mapsto [1, y, z] = [1, -s^2, s^3],$$

from which we can get

$$\begin{aligned} \frac{1}{\pi(s)} - \frac{1}{\pi(p_2)} &= \frac{z(s)}{1} - \frac{1}{\infty} \propto s^3 \Rightarrow \nu_{p_2}(\pi) = 3, \\ \omega &= y(s)d\left(\frac{1}{z(s)}\right) \propto \frac{ds}{s^2} \Rightarrow \nu_{p_2}(\omega) = -2. \end{aligned}$$

3. Near $q_{ab} = [t_{2ab}, v_{2a}, 1]$, the Newton polygon of $F(t_{2ab} + x, v_{2a} + y, 1)$ is shown in Figure 48. This gives us a polynomial

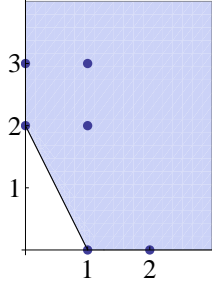


Figure 48: Newton polygon of $F(t_{2ab} + x, v_{2a} + y, 1)$

$$\left(2b\sqrt{\left(v_{2a}^3 + \frac{u_3}{2}\right)^2 - 1}\right)x + 3v_{2a}t_{2ab}y^2,$$

whose zero locus is the local representation of \bar{C}_{SW} at $x = y = 0$. The local normalization near q_{ab} is

$$\begin{aligned} \sigma : s \mapsto [t_{2ab} + x, v_{2a} + y, 1] &= [t_{2ab} + s^2, v_{2a} + c_0s, 1], \\ c_0 &= \sqrt{-\frac{2b}{3v_{2a}t_{2ab}}\sqrt{\left(v_{2a}^3 + \frac{u_3}{2}\right)^2 - 1}}. \end{aligned}$$

from which we can get

$$\begin{aligned} \pi(s) - \pi(q_{ab}) &= \frac{t_{2ab} + x(s)}{1} - t_{2ab} \propto s^2 \Rightarrow \nu_{q_{ab}}(\pi) = 2, \\ \omega &= \frac{v_{2a}}{t_{2ab}}d(x(s)) \propto sds \Rightarrow \nu_{q_{ab}}(\omega) = 1. \end{aligned}$$

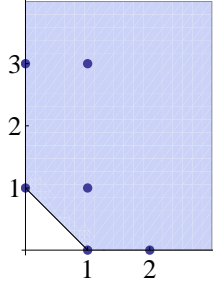


Figure 49: Newton polygon of $F(t_{3\pm} + x, y, 1)$

4. Near $r_{\pm} = [t_{3\pm}, 0, 1]$, the Newton polygon of $F(t_{3\pm} + x, y, 1)$ is shown in Figure 49. This gives us a polynomial

$$2 \left(t_{3\pm} - \frac{u_3}{2} \right) x - u_2 t_{3\pm} y,$$

whose zero locus is the local representation of \bar{C}_{SW} at $x = y = 0$. The local normalization near r_{\pm} is

$$\sigma : s \mapsto [t_{3\pm} + x, y, 1] = [t_{3\pm} + s, d_0 s, 1], \quad d_0 = \frac{1}{u_2} \left(2 - \frac{u_3}{t_{3\pm}} \right).$$

from which we can get

$$\begin{aligned} \pi(s) - \pi(r_{\pm}) &= \frac{t_{3\pm} + x(s)}{1} - t_{3\pm} \propto s \Rightarrow \nu_{r_{\pm}}(\pi) = 1, \\ \omega &= \frac{y(s)}{t_{3\pm}} d(x(s)) \propto s ds \quad \Rightarrow \nu_{r_{\pm}}(\omega) = 1. \end{aligned}$$

From these results we can find out

$$\begin{aligned} R_{\pi} &= 2 \cdot [p_1] + 2 \cdot [p_2] + 1 \cdot [q_{++}] + 1 \cdot [q_{+-}] + 1 \cdot [q_{-+}] + 1 \cdot [q_{--}], \\ (\omega) &= -2 \cdot [p_1] - 2 \cdot [p_2] + 1 \cdot [q_{++}] + 1 \cdot [q_{+-}] + 1 \cdot [q_{-+}] + 1 \cdot [q_{--}] + 1 \cdot [r_+] + 1 \cdot [r_-]. \end{aligned}$$

References

- [1] E. Witten, *Solutions of four-dimensional field theories via M- theory*, *Nucl. Phys.* **B500** (1997) 3–42, [[hep-th/9703166](#)].
- [2] N. Seiberg and E. Witten, *Monopole Condensation, And Confinement In N=2 Supersymmetric Yang-Mills Theory*, *Nucl. Phys.* **B426** (1994) 19–52, [[hep-th/9407087](#)].
- [3] N. Seiberg and E. Witten, *Monopoles, duality and chiral symmetry breaking in N=2 supersymmetric QCD*, *Nucl. Phys.* **B431** (1994) 484–550, [[hep-th/9408099](#)].
- [4] D. Gaiotto, *N=2 dualities*, [arXiv:0904.2715](#).

- [5] P. C. Argyres and N. Seiberg, *S-duality in $N=2$ supersymmetric gauge theories*, *JHEP* **12** (2007) 088, [[arXiv:0711.0054](https://arxiv.org/abs/0711.0054)].
- [6] P. C. Argyres and M. R. Douglas, *New phenomena in $SU(3)$ supersymmetric gauge theory*, *Nucl. Phys.* **B448** (1995) 93–126, [[hep-th/9505062](https://arxiv.org/abs/hep-th/9505062)].
- [7] F. Kirwan, *Complex Algebraic Curves*. Cambridge University Press, 1992.
- [8] P. A. Griffiths, *Introduction to Algebraic Curves*. American Mathematical Society, 1989.
- [9] M. Kerr, *Lecture Notes on Algebraic Geometry*.
<http://www.maths.dur.ac.uk/~dma0mk/AGbook.pdf>.
- [10] A. Fayyazuddin and M. Spalinski, *The Seiberg-Witten differential from M-theory*, *Nucl. Phys.* **B508** (1997) 219–228, [[hep-th/9706087](https://arxiv.org/abs/hep-th/9706087)].
- [11] M. Henningson and P. Yi, *Four-dimensional BPS-spectra via M-theory*, *Phys. Rev.* **D57** (1998) 1291–1298, [[hep-th/9707251](https://arxiv.org/abs/hep-th/9707251)].
- [12] A. Mikhailov, *BPS states and minimal surfaces*, *Nucl. Phys.* **B533** (1998) 243–274, [[hep-th/9708068](https://arxiv.org/abs/hep-th/9708068)].
- [13] P. C. Argyres, M. Ronen Plesser, N. Seiberg, and E. Witten, *New $N=2$ Superconformal Field Theories in Four Dimensions*, *Nucl. Phys.* **B461** (1996) 71–84, [[hep-th/9511154](https://arxiv.org/abs/hep-th/9511154)].